DOI:10.1016/j.enconman.2018.09.082

Study of the energetic needs for the on-board production of Oxy-Hydrogen as fuel additive in internal combustion engines

Pierpaolo Polverino[a,*], Federica D'Aniello[a], Ivan Arsie[a], Cesare Pianese[a]

[a]*Department of Industrial Engineering, University of Salerno, via Giovanni Paolo II 132, 84084, Fisciano (SA), ITALY.*

Abstract

The present study aims at assessing, from a theoretical point of view, the feasibility of on-board production and use of Oxy-Hydrogen (HHO) as fuel additive in internal combustion engines. From the available literature, many works deal with the experimental investigation of the benefits achieved with HHO use in both compression and spark ignition engines in terms of brake thermal efficiency improvement and emissions reduction. Nevertheless, a thorough demonstration of the feasibility of HHO on-board production and use has not been performed yet, also due to the unclear nature of the generated HHO mixture. To bridge this gap, a rigorous analysis of the energetic needs related to HHO production through electrolysis, with the internal combustion engine as unique power supply, is here described in details. An innovative assumption is proposed to achieve a generalized representation of HHO mixture and univocally determine the energetic requirements related to its production. A conventional layout is considered to

*Corresponding author
Email address: ppolverino@unisa.it (Pierpaolo Polverino)
URL: www.eprolab.unisa.it (Pierpaolo Polverino)

define realistic restrictions for HHO use and fuel savings achievement. Several case studies, based on works available in the literature, are investigated to prove the validity of the proposed analysis and assess the feasibility of the technological approach.
Keywords: HHO, Energetic Analysis, Fuel Savings, Engines, Automotive, Electrolysis.

---

1. Introduction

In the last years, the increase in fuel costs and the alarming environmental issues made the governing bodies of several countries implement severe regulations to lower pollutant emissions and improve the use of renewable energy sources. Large efforts have been performed by researchers and industries to develop unconventional and more efficient power generation systems, to reduce the dependency on fossil fuels and decrease harmful emissions, especially in urban environment.

Great attention is drawn, for instance, by batteries and fuel cells in automotive applications. However, their spread in the worldwide market is still hindered by several problems (if compared to conventional systems): i) high costs of materials and manufacturing processes, ii) low range, durability and reliability, iii) limited availability of dedicated refuelling stations. Therefore, Internal Combustion Engines (ICEs) will be still predominant in private and public transportation at least for the next two decades.

The improvement of engine efficiency and the use of alternative fuels are playing a key role in emissions reduction. Indeed, Compressed Natural Gas (CNG), Liquefied Petroleum Gas (LPG), biodiesels, alcohols (e.g., methanol and ethanol) and hydrogen are considered cleaner and more environmental friendly fuels if

compared to gasoline and Diesel [1]. Among them, hydrogen has been considered quite attractive for its unique features, especially if used as fuel additive [2].

Hydrogen is fully renewable, recyclable and non-pollutant [3]. It has a wide flammability range (from 4% to 75% volume in air) and low ignition energy (0.02 mJ), which allows running engines at large air/fuel ratios and lean mixtures [4]. Hydrogen shows high flame speed and high diffusivity, which improve mixture uniformity and prompt ignition [5]. Moreover, it has high octane rating, auto ignition temperature (585 °C) and specific energy content (142.18 MJ/kg as Higher Heating Value (HHV) and 120.21 MJ/kg as Lower Heating Value (LHV) [6]).

Thanks to these properties, various improvements in engines operation can be achieved. For instance, larger compression ratio can be adopted [5], while lower cylinder peak temperatures and pressures are achieved under extreme lean mixtures [7]. Moreover, the more uniform mixing of air and fuel, combined with the sudden and rapid combustion, enhances, on the one hand, the overall thermal efficiency, and reduces, on the other hand, engine emissions [2].

In the work of de Morais et al. [7], the effects obtained by using pure hydrogen as partial substitute in a Diesel power generator are investigated. The chosen engine presented the following features: four cylinders, direct injection, 3922 cc and 50 kW (@ 2800 rpm) of nominal power. The authors kept the engine unmodified, but equipped the fuel intake with a hydrogen injection system, controlled through a dedicated Electronic Control Unit (ECU). Various hydrogen flow rates (that allowed to replace from 5% to 20% of Diesel fuel on energy basis) were tested at different loads (from 0 kW to 40 kW), achieving a fuel consumption reduction of about 16% at high concentrations and loads, although no significant changes in Specific Fuel Consumption (SFC) or air to fuel ratio were noticed over the whole

range. Nonetheless, a reduction in CO_2 emissions up to 12% was observed.

It is worth noting that hydrogen might not be used as sole fuel in Compression Ignition (CI) engines, since it is difficult to reach auto ignition temperature, thus requiring a spark plug [4]. Knocking and detonation, as well as backfire, flashbacks and pre-ignitions issues, not desirable in Spark Ignition (SI) engines, can also occur [5]. Furthermore, the low density of hydrogen requires on-board storage at high pressures, with related safety issues.

To overcome all these problems, a solution can be found in the direct on-board production of hydrogen, through, e.g., electrolyser units, thus reducing storage. Electrolysis is a widely renown methodology through which hydrogen and oxygen gases are produced from water by providing voltage or current to the electrolyser unit [8]. A direct mixture of hydrogen and oxygen is known in the literature as Oxy-Hydrogen (HHO) or Brown's Gas [6]. Such mixture has been widely analysed by several researchers to investigate efficiency improvements and emissions reduction in both CI [3, 9, 10, 11] and SI [12, 13, 14] engines.

Noteworthy is the work of Yilmaz et al. [4], who tested the use of HHO as additive fuel to a four cylinder, direct injection, 3567 cc CI engine, with a maximum brake power of 80 kW at 1800 rpm. HHO was generated by means of an in-house-made electrolyser unit (powered with an external supply), and its injection at the intake manifold was regulated by a dedicated ECU. Various engine speeds were tested (from 1200 rpm to 2800 rpm) and the injected amount of HHO was changed accordingly. An average increase of 19.1% in engine torque and an average gain of 14% in SFC were observed. Moreover, HC and CO emissions were lowered of about 5% and 13.5%, respectively.

On the same line, Bari et al. [2] investigated the efficiency gain and emissions

reduction of an unmodified four cylinder, direct injection, 4010 cc Diesel engine, under the addition of several amounts of HHO. Three power levels (19 kW, 22 kW and 28 kW), at constant speed of 1500 rpm, and HHO flow rates up to 30 LPM were tested, with HHO produced with a commercial HHO generator (Epoch EP-500). The authors observed a maximum increase in Brake Thermal Efficiency (BTE) of 8.8%, with a corresponding reduction in SFC of 8.1%. Moreover, HC, CO and CO_2 emissions were diminished, while NOx increased (due to peak pressures and temperatures related to the high energy content and flame speed of HHO).

Also Premkartikkumar et al. [1] analysed the effects of HHO addition to a single cylinder, direct injection, Diesel engine (rated power of 5.9 kW at 1800 rpm), with HHO produced with an in-house-made generator, powered with an external 12 V source. The engine was tested under different loads and with HHO flow rate from 1 LPM up to 3.3 LPM, whereas the effects of injection time was further analysed in a subsequent work [15]. As observed by other researchers [2, 4, 12], the effects of HHO addition change upon engine operation and injected amount. Therefore, in some cases, a significant improvement can be only achieved by proper regulation of HHO injection and engine operation. The cited authors indeed observed an increase in BTE of 11.06% at 100% rated load and 3.3 LPM of HHO, while a reduction of 4.15% was obtained at 25% rated load and 1 LPM of HHO. With respect to emissions, at high loads and HHO flow rates, CO, HC and smoke decreased, while CO_2 and NOx increased (conversely at low loads and HHO flow rates).

Arat et al. [6] studied the performance of an unmodified, four cylinder, direct injection, 3567 cc Diesel engine enriched, on the one hand, with only HHO (5.14 LPM) and, on the other hand, with a mix of HHO and CNG (5.14 LPM and 15.36

LPM, respectively), both with pilot Diesel injections. HHO was generated with an in-house-made device, powered by a 24 V battery, and the tests were performed varying engine speed between 1200 rpm and 2600 rpm. With sole HHO as additive, BTE increased of about 3.4% whereas SFC decreased of 17.4%. The use of HHO and CNG improved previous results: BTE raised of 6.28% and SFC lowered of 27.2%. In all cases, both CO_2 and NOx decreased (probably due to less air intake), while CO increased in the former case and decreased in the latter.

The aforementioned works confirmed the validity of using HHO as fuel additive to improve both performance and emissions of ICEs. However, their practical use in automotive applications require on-board powering of HHO production devices. Many authors account for the possibility to supply energy to HHO electrolysers through vehicle batteries [2, 6, 10, 11, 13], but their performance and, thus, power request depend on the chosen materials and configurations.

Manu et al. [9] performed an experimental analysis to find the optimal setup for HHO production through a dry electrolyser. The authors adopted a design of experiment technique to investigate four different factors: i) space between electrodes (2 mm and 3 mm), ii) electrolyte type (NaOH and KOH), iii) electrolyte concentration (20% and 30%) and iv) electrodes surface roughness (smooth and rough). They found that the best configuration (with 316-L stainless steel electrodes) was with KOH at 30% and with rough electrodes spaced 3 mm. Afterwards, this configuration was considered during tests with a single cylinder, 553 cc CI engine at different HHO flow rates (0.89 LPM, 1.37 LPM, 1.66 LPM and 2 LPM), obtaining an increase in BTE and a decrease in the related SFC.

Also Masjuki et al. [11] tested HHO electrolyser performance with different number of electrodes (2 and 3), KOH catalyst concentration (0.5% and 1%) and

electrodes gap (10 mm and 50 mm), achieving an optimal design with 3 electrodes spaced 50 mm and with 1% of KOH. Then, the addition of HHO to a single cylinder, direct injection, 815 cc Diesel engine was studied at different engine speeds (from 1200 rpm to 2000 rpm), achieving also in this case a visible gain in power and SFC saving, with a reduction of CO and HC and an increase in NO.

Recently, Ismail et al. [16] tested three in-house-made dry cell electrolysers to provide a 1498 cc CI engine with a constant amount of HHO (0.375 LPM). The electrolysers were designed changing voltage and current operation, amount of catalyst (NaOH), number and area of electrodes and stacks. The authors equipped the engine also with a dedicated ECU to control oxygen inlet, so as to ensure fuel savings (which may not be achieved otherwise). Once assessed the best configuration, they investigated the improvements in BTE, SFC and engine emissions.

From the investigated literature, it can be noticed that many authors focused on the enhancement of electrolysers performance and the analysis of engines improvements by using HHO as fuel additive. However, a thorough demonstration of the feasibility of running such devices on-board for automotive uses is still missing. This work aims at performing a rigorous analysis of the energetic needs related to HHO production through electrolysis, with the engine as main power supply for the electrolyser. In the following sections, the energetic needs related to HHO production are analysed first, followed by an overview on the considered system configuration and the corresponding restrictions, to define the limits for realistic fuel saving conditions. Then, several case studies, based on chosen works addressed in the literature survey, are investigated to prove the validity of the proposed analysis and assess the feasibility of the technological approach.

2. Energetic needs for HHO production

Hydrogen production can be performed by means of different methodologies, such as gas reforming or water electrolysis, but this latter represents the most suitable method to produce hydrogen with high purity with a rather high efficiency. Water electrolysis is usually performed by providing energy to split water molecules into their components, i.e. hydrogen and oxygen. This process can occurr either at high or low temperatures, through the use of specific electrolytes and ionic agents. Therefore, electrolysers can be generally classified in alkaline, polymer electrolyte membrane, and solid oxide ones [8].

2.1. Water electrolysis reaction

Due to their low operating temperature and production cost, as well as their easy manufacturing and management, alkaline electrolysers have been preferred for HHO applications by most of the works available in the literature [4, 6, 9, 10, 11, 13, 14, 16, 17]. These type of electrolysers are generally characterized by two or more electrodes (usually made of 316-L stainless steel plates) immersed in distilled water with a dissolved electrolyte (e.g., NaOH or KOH), which promotes the reaction. The water molecules are split thanks to a potential difference imposed to the electrodes edge and the overall electrochemical reaction is:

$$2H_2O \rightarrow 2H_2 + O_2$$

This reaction expresses that for each mole of consumed water, one mole of hydrogen and half a mole of oxygen are produced. Moreover, it is essentially composed by the Oxygen Evolution Reaction (OER), occurring at anode side (positive electrode), and the Hydrogen Evolution Reaction (HER), taking place at cathode side (negative electrode) [8, 17]:

$$4OH^- \rightarrow 2H_2O + O_2 + 4e^- \text{ (OER)}$$
$$4H_2O + 4e^- \rightarrow 4OH^- + 2H_2 \text{ (HER)}$$

The reactions evolves through different pathways, with production of intermediate elements [17]. Particularly, the HER is firstly characterized by the Volmer reaction:

$$H_2O + e^- \rightarrow H_{ads} + OH^- \text{ (Volmer)}$$

where hydrogen atoms H_{ads} are generated. This reaction represents the rate determining step of the whole HER at low potential. Afterwards, either the Heyrovsky or Tafel processes (the former electrochemical, while the latter chemical) can take place [8]:

$$H_{ads} + H_2O + e^- \rightarrow H_2 + OH^- \text{ (Heyrovsky)}$$
$$2H_{ads} \rightarrow H_2 \text{ (Tafel)}$$

The analysis of the former processes clarifies how the production steps of water electrolysis involves more elements rather than only hydrogen and oxygen molecules, particularly hydrogen atoms as intermediate products. This aspect is fundamental to support the assumptions made on HHO nature in Section 2.3.

2.2. Electrolysis energy demand

The energy required for water electrolysis can be expressed in terms of specific Gibbs free energy change Δg from reactants to products. Neglecting the entropy change (ideal case) and the effects of temperature, the Gibbs free energy can be expressed in terms of enthalpy variation. Considering and ideal electrolysis process (i.e., with no energy losses), to produce hydrogen from water, the minimum

energy that should be given to the electrolyser corresponds to the overall energy attained by the produced H_2 molecules. Assuming that the water provided to the electrolyser is in liquid state, the variation in enthalpy can be roughly quantified through the hydrogen HHV. Indeed, this value corresponds to the maximum energy potential attained by hydrogen molecules H_2, which can be used through an oxidation reaction (i.e., combustion) by considering water produced in liquid form. Therefore, the minimum energy requested for liquid water electrolysis can be assumed equal to hydrogen HHV.

A given volume V_{H_2O} of distilled water contains n_{H_2O} water moles, which can be converted in the same amount of H_2 moles n_{H_2} (see previous section). The volume V_{H_2} occupied by n_{H_2} depends on the environmental conditions at which the hydrogen is produced and can be evaluated through the ideal gas law, as also suggested by [11]:

$$V_{H_2} = \frac{\bar{R}T}{p} n_{H_2} \tag{1}$$

where $\bar{R}$ is the ideal gas constant, whereas T and p are the reference temperature and pressure respectively. Recalling that:

$$n_{H_2} = n_{H_2O} = V_{H_2O} \frac{\rho_{H_2O}}{M_{H_2O}} \tag{2}$$

equation (1) becomes:

$$V_{H_2} = \frac{\rho_{H_2O}}{M_{H_2O}} \frac{\bar{R}T}{p} V_{H_2O} \tag{3}$$

In equations (2) and (3), the term ρ_{H_2O} and M_{H_2O} are the water density and molar mass, respectively. Assuming Normal Temperature and Pressure (NTP - 20°C and 1 atm) [18] or Standard Temperature and Pressure (STP - 0°C and 1 bar) conditions

[19], the volume of hydrogen produced from 1 L of water (density 1 kg/L and molar mass 18 g/mol) is about 1.336 m^3 (normal) or 1.262 m^3 (standard).

Recalling that hydrogen has a molar mass of 2 g/mol and an HHV of about 142.18 kJ/mol [6], the ideal energy consumption per 1 m^3 of produced hydrogen can be evaluated as:

$$\varepsilon_{H_2} = M_{H_2} \frac{p}{\bar{R}T} HHV_{H_2} \tag{4}$$

which is about 11.82 MJ/m^3 (3.28 kWh/m^3) in NTP and 12.52 MJ/m^3 (3.48 kWh/m^3) in STP. Assuming an electrolyser efficiency between 59% and 70% [8], the average gross request of electrical energy at the electrodes can be estimated as 5.28 kWh/m^3, in line with the estimate of 4.5 kWh/m^3 given by Sapountzi et al. [8].

To express the previous calculations in terms of power demand, the evaluation of the produced hydrogen mass flow $\dot{m}_{H_2}$ should be performed. This can be made considering the Faraday's law, which relates the provided current I to the hydrogen molar flow $\dot{n}_{H_2}$ [11, 14]:

$$\dot{n}_{H_2} = \frac{IN_c}{2F} \tag{5}$$

where F is the Faraday's constant and N_c is the number of the electrolyser cells. This equation links the electronic charge of 2 moles of electrons to each mole of produced H_2 (see HER). Hydrogen volumetric flow can be expressed by using $\dot{n}_{H_2}$ instead of n_{H_2} in equation (1):

$$\dot{V}_{H_2} = \frac{\bar{R}T}{p} \frac{IN_c}{2F} \tag{6}$$

Therefore, at a given current, the related power requested for a certain hydrogen volumetric flow is:

$$P^{r}_{H_2} = \varepsilon_{H_2}\dot{V}_{H_2} = M_{H_2}\frac{IN_c}{2F}HHV_{H_2} \tag{7}$$

From equation (7), the ideal power consumption for H_2 production seems not to depend directly on the operating conditions (i.e., temperature and pressure). However, it is worth reminding that this calculation represents the net power consumption, without entailing electrolyser efficiency. This latter is indeed strictly dependent on the working conditions, thus influencing the gross power at electrolyser inlet in terms of voltage and current.

The previous reasoning is based on the evaluation of the produced hydrogen amount, but since this study entails Oxy-Hydrogen, the required energy estimation should be made directly on HHO.

2.3. Definiton of HHO

Oxy-Hydrogen is usually defined as a stoichiometric mixture of 2/3 of hydrogen and 1/3 of oxygen (by volume) obtained from water electrolysis, but its nature is still unclear. Some works relate the molar fractions to hydrogen and oxygen in their diatomic state (i.e., H_2 and O_2) [2, 3, 6, 16], while other works claim that they appear in their monoatomic state [4, 11, 10].

According to these latter, HHO is described as an unstable state of the water, where no atomic bonds are needed to be broken before turning back hydrogen and oxygen into water. When HHO is ignited in the engine combustion chamber, it is assumed that both explosion and implosion occur. The cited works claim that pulverized water aggregates with fuel particles becoming a binary mixture, with

water being the core and the fuel the shell (due to density differences). The increase in heat and pressure leads the water to vaporize, with a consequent atomization of the fuel and a better mixing with surrounding oxygen.

A more advanced study of HHO was made by Santilli [20], who proposed a peculiar explanation of the monoatomic structure of oxy-hydrogen. In this work, HHO is explicitly distinguished from the conventional Brown's gas definition of a mixture characterized by diatomic molecules of hydrogen and oxygen. The author investigated several molar masses measurements, underlying the presence in the mixture of single atoms of oxygen (16 amu) in addition to water vapour (18 amu), oxygen molecules (32 amu) and other heavier elements (up to 40 amu). Nevertheless, the presence of single hydrogen atoms was highly expected, although not confirmed by the experiments since the instrumentations were not capable to measure 1 amu elements.

The proper definition of HHO composition is not univocal and can change the evaluation of the related molar flow and weight. Therefore, to determine a generalized representation of HHO mixture, the following assumptions are considered: first of all, the presence of other species rather than hydrogen and oxygen is neglected, their moles ratio is assumed stoichiometric (i.e., 2:1) and they are considered both in diatomic and monoatomic state. This latter statement is supported by the analysis of water electrolysis reactions made in Section 2.1.

According to these assumptions, the representation of HHO composition is expressed as follows:

$$\mathrm{HHO} = \frac{2}{3}\Big[\zeta \mathrm{H_2} + (1-\zeta)\mathrm{H}\Big] + \frac{1}{3}\Big[\zeta \mathrm{O_2} + (1-\zeta)\mathrm{O}\Big] \tag{8}$$

where ζ is a parameter representing the hydrogen and oxygen diatomic state

fraction: if only diatomic molecules are considered, then $\zeta = 1$, whereas $\zeta = 0$ in case of purely monoatomic mixture. In general, the state fractions for H_2 and O_2 could differ, but they are here assumed being the same, to keep a stoichiometric ratio for both diatomic and monoatomic states. Intermediate values represent a mixture of elements in both states.

Assuming that an amount of elements in monoatomic state can be considered equivalent to an halved amount in diatomic state, equation (8) becomes:

$$\mathrm{HHO} = x_{H_2}\mathrm{H}_2 + x_{O_2}\mathrm{O}_2 \tag{9}$$

where x_{H_2} and x_{O_2} are the molar fractions of hydrogen and oxygen, respectively, and are equal to:

$$x_{H_2} = \frac{1+\zeta}{3} \tag{10}$$

$$x_{O_2} = \frac{1+\zeta}{6} \tag{11}$$

Therefore, HHO molar weight can be calculated as follows:

$$M_{HHO} = x_{H_2}M_{H_2} + x_{O_2}M_{O_2} \tag{12}$$

Considering that $M_{H_2} \approx 2$ g/mol and $M_{O_2} \approx 32$ g/mol, Table 1 resumes some of the aforementioned HHO properties according to pure diatomic or pure monoatomic state assumption.

The amount of HHO moles can be thus estimated upon the knowledge of the related hydrogen moles amount as follows:

Table 1: Properties of HHO in pure diatomic and monoatomic states.

	Pure diatomic	**Pure monoatomic**
ζ [-]	1	0
x_{H_2} [-]	2/3	1/3
x_{O_2} [-]	1/3	1/6
M_{HHO} [g/mol]	12	6

$$n_{HHO} = \frac{n_{H_2}}{x_{H_2}} \tag{13}$$

From the above comments, it is clear that a precise definition of the HHO mixture is fundamental for the estimation of proper correlation with hydrogen moles, necessary for the estimation of the energy requirements with respect to a given HHO volumetric flow, as illustrated in the following.

2.4. HHO power request analysis

From equation (13), the mass of H_2 available in a unit mass of HHO is:

$$m_{H_2} = \frac{M_{H_2}}{M_{HHO}} x_{H_2} m_{HHO} \tag{14}$$

and the specific energy of HHO can be then assumed as the equivalent energy of H_2 within a unit mass of HHO:

$$HHV_{HHO} = \frac{M_{H_2}}{M_{HHO}} x_{H_2} HHV_{H_2} \tag{15}$$

Combining equations (2) and (8) and considering that equation (1) can apply also to HHO, the volume of HHO produced from a given amount of distilled water can be evaluated as:

$$V_{HHO} = \frac{V_{H_2O}}{x_{H_2}} \frac{\rho_{H_2O}}{M_{H_2O}} \frac{\bar{R}T}{p} = \frac{V_{H_2}}{x_{H_2}} \tag{16}$$

and the ideal energy consumption per 1 m^3 of produced HHO is:

$$\varepsilon_{HHO} = x_{H_2} M_{H_2} \frac{p}{\bar{R}T} HHV_{H_2} = x_{H_2} \varepsilon_{H_2} \tag{17}$$

which is about 7.88 MJ/m^3 (2.19 kWh/m^3) in NTP and 8.35 MJ/m^3 (2.32 kWh/m^3) in STP for pure diatomic state, and about 3.94 MJ/m^3 (1.09 kWh/m^3) in NTP and 4.17 MJ/m^3 (1.16 kWh/m^3) in STP for pure monoatomic state. Faraday's law is still valid and can be expressed with respect to HHO volumetric flow combining equations (6) and (16):

$$\dot{V}_{HHO} = \frac{\bar{R}T}{p} \frac{IN_c}{2Fx_{H_2}} \tag{18}$$

The previous equation correlates HHO production to the current provided to the electrolyser. Moreover, the same approach expressed in equation (7) can be also applied to compute HHO production power demand:

$$P^r_{HHO} = \varepsilon_{HHO} \dot{V}_{HHO} \tag{19}$$

Through equation (19), given a certain HHO volumetric flow, the ideal power requested to the electrolyser is then obtained. However, recalling equation (17):

$$P^r_{HHO} = x_{H_2} \varepsilon_{H_2} \frac{\dot{V}_{H_2}}{x_{H_2}} = P^r_{H_2} \tag{20}$$

This result is quite straightforward considering that the power provided to the electrolyser should not depend on the representation of HHO state (either diatomic, monoatomic or a combination of the two) but only on the energy needs related

to the involved electrochemical reactions and the overall equivalent amount of produced hydrogen.

2.5. HHO power request verification

The equations introduced in the previous sections are here verified with respect to experimental data taken from the literature. Among the analysed works, that of Ismail et al. [16] presents the most complete data set related to electrolyser performance testing. As described in Section 1, three different dry electrolysers have been designed and built to investigate the best configuration for HHO production. Once identified the most performing one, a series of tests at different amounts of NaOH have been carried out measuring voltage, current, water temperature and produced HHO flow. These measurements have been collected at the start of the electrolysis process (0 min) and after 90 min, when the steady-state is considered reached. A graphical representation of the electrolyser current and water temperature as well as the related HHO volumetric flow measurements gathered by Ismail et al. [16] are here reported in Figure 1 and Figure 2, respectively. Current and temperature are represented as function of time and NaOH amount, whereas HHO flow as function of the measured current. The parameters values considered for the energetic verification with respect to these data are resumed in Table 2.

Using the data presented in Table 2 and Figure 1 as inputs, equation (18) is now applied to estimate the HHO volumetric flow in pure diatomic and pure monoatomic states. The results are presented in Figure 3-a in comparison with the measured HHO flow already reported in Figure 2. For the sake of simplicity, the measurements reported in Figure 2 are here sketched with only square blue markers, whereas the estimations in pure diatomic and pure monoatomic states are reported in dashed red line and diamond marker, the former, and dashed yellow

Table 2: Parameters considered for the energetic verification based on the work of Ismail et al. [16].

Parameter	Value	Unit	Reference
HHV_{H_2}	142.18	MJ/kg	[6]
$\bar{R}$	8.314472	J/mol/K	[11]
F	96485.34	C/mol	[11]
p	$1.01325 \cdot 10^5$	Pa	[16]
N_c	6	-	[16]
V	13.8	V	[16]

line and circle marker, the latter. A significant result is here achieved since all the measurements fall within the two boundaries delimited by pure diatomic and pure monoatomic states.

This evidence confirms the correct representation of HHO as a mixture composed by a variable amount of elements in both states. It can be observed that at low currents, the mixture behave more similarly to a pure diatomic mixture, whereas a greater amount of monoatomic elements seems to appear at higher currents.

The electric power required for the HHO production is then evaluated through equation (19) considering the HHO volumetric flow measurements (Figure 2) as input and computing the ideal energy consumption through equation (17) for both pure diatomic and pure monoatomic states. The results are shown in Figure 3-b and compared to the provided battery power (see Table 2 and Figure 1-a for measured voltage and current values) and the required power evaluated through equation (20) (i.e., based on Faraday's law as detailed in equation (7) and represented through a dashed black line with triangular markers).

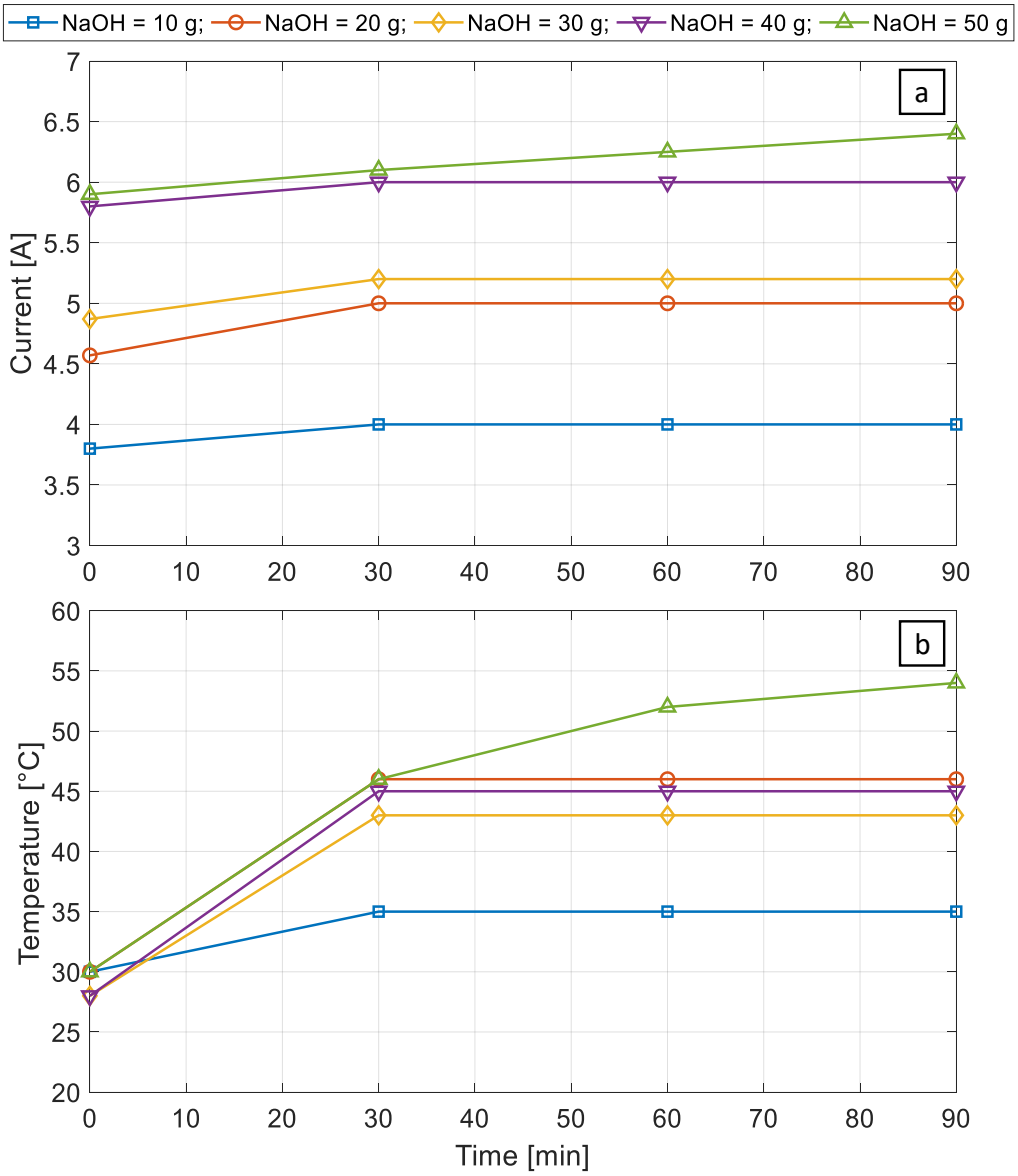

Figure 1: Graphical representation of the electrolyser current (a) and water temperature (b) measurements reported by Ismail et al. [16] with respect to operating time and NaOH amount.

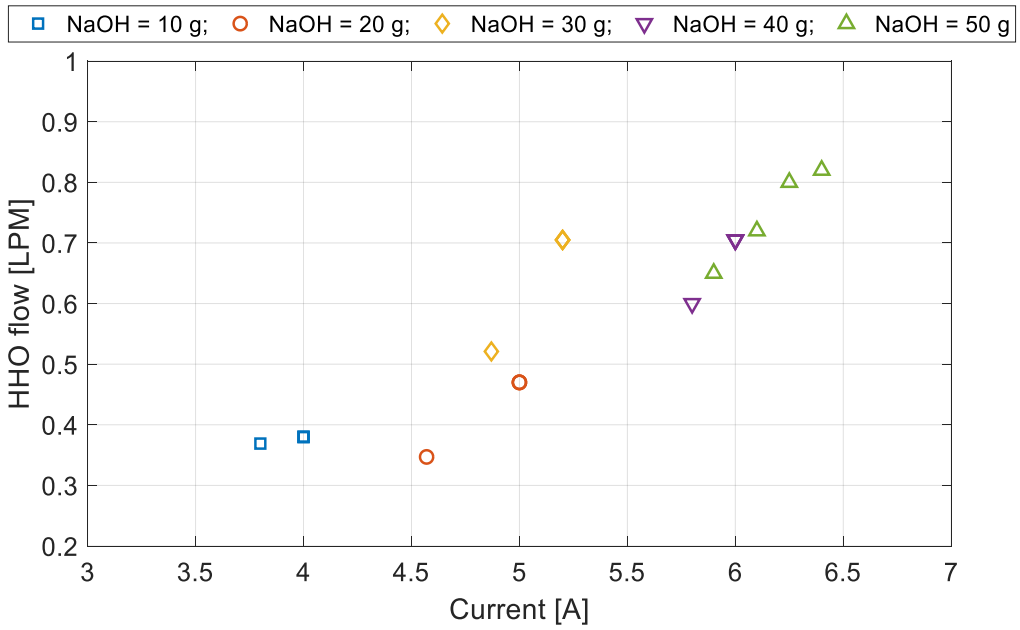

Figure 2: Graphical representation of the HHO volumetric flow measurements reported by Ismail et al. [16] with respect to electrolyser current (illustrated in Figure 1-a).

It can be observed that the use of Faraday's law univocally identifies a power request coherent with the power provided by the battery, showing an efficiency of 64% perfectly in agreement with what stated in Section 2.2 and reported by Sapountzi et al. [8]. The power estimation made through pure monoatomic state assumption could underestimates the real power request, whereas an overestimation is instead achieved with pure diatomic state assumption (with the consumption sometimes higher that the provided power, which is not realistic). This result confirms again the behaviour of the mixture as a combination of diatomic and monoatomic states of hydrogen and oxygen.

The former verification confirms the validity of the proposed analysis in assessing the power request for HHO production through electrolysis. In the following

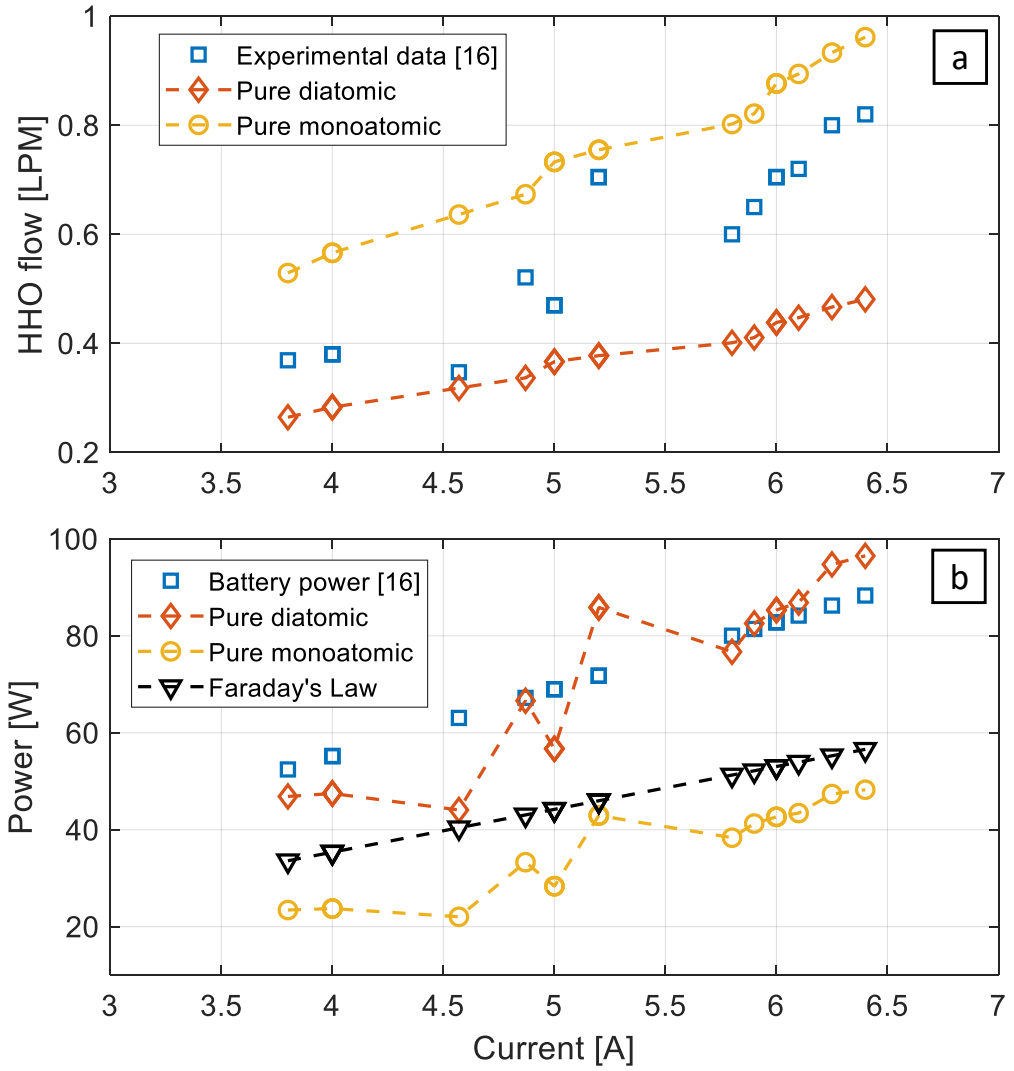

Figure 3: HHO volumetric flow (a) and electrolyser power request (b) estimations in both pure diatomic and pure monoatomic states, compared with the measurements performed by Ismail et al. [16].

section, the energetic investigation is extended including the electrolysers within a typical automotive configuration, with the engine as main power generator.

3. Energetic Analysis of on-board HHO production

The system layout considered in this work is sketched in Figure 4 and has been adapted from a preliminary study recently published by the authors [21]. The accounted configuration is designed starting from the same layout available on conventional vehicles, adapted according to schemes also addressed in the literature [1, 2, 4, 5, 6, 9, 12, 13, 14, 16]. The system here considered is composed of four main components: an engine (ICE), either CI or SI, an Electric Motor Generator (EMG), a battery, an electrolyser, a mechanical load, a fuel tank and a water tank. The fuel tank and the electrolyser provide the engine with the chemical power attained by the fuel flow $\dot{m}_f$ (either Diesel, gasoline, or any other fuel) and the HHO flow $\dot{m}_{HHO}$. The engine converts the provided chemical power in mechanical power available at the main shaft. This power is then used to fulfil the load request and to power the EMG, thanks to mechanical transmissions. The EMG converts the mechanical power into electric power, to charge the battery. This latter is used to feed the vehicle auxiliaries and also the electrolyser, which uses the provided electric power to convert the inlet water flow $\dot{m}_{H_2O}$ into HHO outlet flow $\dot{m}_{HHO}$.

All the power (or, as well, energy) conversions described above involve losses, according to the performance of each considered component. Therefore, a simple evaluation of the required fuel flow can be defined upon the knowledge of the power request at the engine main shaft and components efficiencies, as described in the following section.

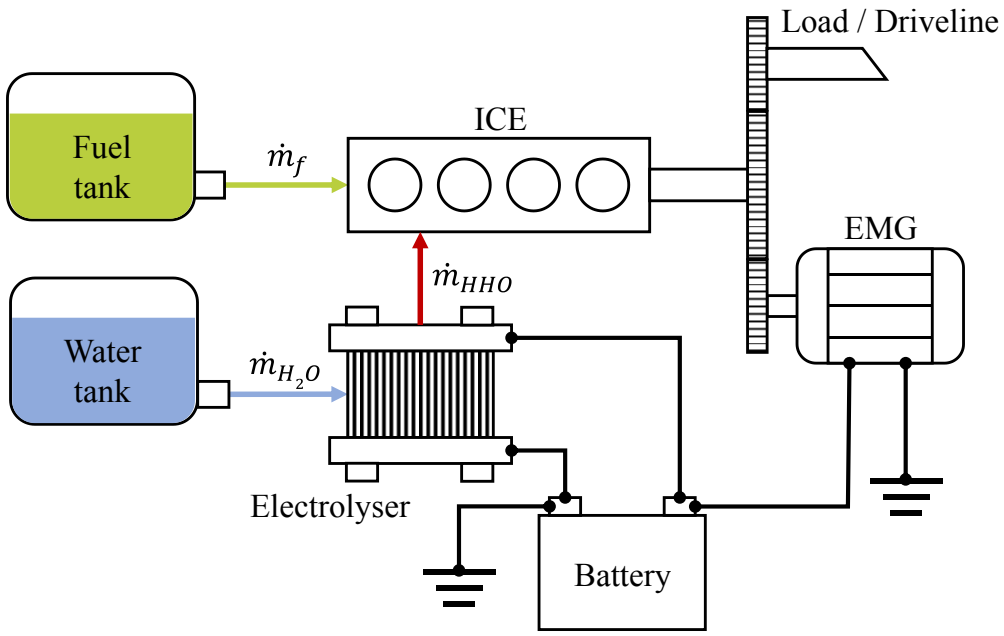

Figure 4: System layout, adapted from [21].

3.1. Fuel consumption evaluation

The chemical power P_{chem} at the engine inlet can be expressed as:

$$P_{chem} = P_f + P_{HHO} \tag{21}$$

where P_f and P_{HHO} are the chemical powers attained by the fuel flow and the HHO flow, respectively:

$$P_f = \dot{m}_f LHV_f \tag{22}$$

$$P_{HHO} = \dot{m}_{HHO} LHV_{HHO} \tag{23}$$

In equations (22) and (23) the terms LHV_f and LHV_{HHO} are the LHV of fuel, the former, and of HHO, the latter.

The engine brake power P_{ICE} can be expressed recalling the definition of Brake Thermal Efficiency (BTE) η_{ICE} as the ratio between the brake power and the inlet chemical power [6, 1, 7]:

$$P_{ICE} = P_{chem} \eta_{ICE} \tag{24}$$

This power amount is immediately available at the main shaft, to cover the load request P_L and the EMG gross power P^g_{EMG}:

$$P_{ICE} = P_L + P^g_{EMG} \tag{25}$$

This latter depends on the gross power needed by the battery P^g_{BATT} to cover the gross power request at the electrolyser P^g_{ELEC}:

$$P^g_{EMG} = \frac{P^g_{BATT}}{\eta_{EMG}} \tag{26}$$

$$P^g_{BATT} = \frac{P^g_{ELEC}}{\eta_{BATT}} \tag{27}$$

where the terms η_{EMG} and η_{BATT} are the EMG and battery efficiencies, respectively.

To produce the amount of HHO $\dot{m}_{HHO}$, the gross power consumption at the electrolyser can be expressed upon knowledge of the HHO production power request P^r_{HHO} and electrolyser efficiency η_{ELEC} :

$$P^g_{ELEC} = \frac{P^r_{HHO}}{\eta_{ELEC}} \tag{28}$$

By combining equations (5), (14) and (15), the term P^r_{HHO} can be expressed as:

$$P^r_{HHO} = \dot{m}_{HHO} HHV_{HHO} \tag{29}$$

where the term HHV_{HHO} is the HHV of the HHO (see equation (15)). Defining α as the ratio between hydrogen LHV and HHV and considering that equation (14) holds also for LHV values, the following relationship between HHO chemical power used in the engine and power request for HHO production is obtained:

$$P_{HHO} = \dot{m}_{HHO} \alpha HHV_{HHO} = \alpha P^r_{HHO} \tag{30}$$

Combining equations (26), (27) and (28), the gross power request at the EMG can be finally expressed in terms of the required power for HHO production:

$$P^g_{EMG} = \frac{P^r_{HHO}}{\eta_{ELEC}\eta_{BATT}\eta_{EMG}} = \frac{P^r_{HHO}}{\eta_{aux}} \tag{31}$$

where η_{aux} is the overall efficiency of the auxiliaries used for HHO production.

The amount of fuel flow required by engine operation can be now evaluated by introducing equations (21), (22), (24), (30) and (31) in equation (25):

$$\dot{m}_f = \frac{P_L}{LHV_f \eta_{ICE}} + \frac{P^r_{HHO}}{LHV_f}\left(\frac{1}{\eta_{ICE}\eta_{aux}} - \alpha\right) \tag{32}$$

Without the use of HHO (or any other additive) during engine operation, the achieved fuel consumption $\dot{m}^0_f$ can be evaluated as:

$$\dot{m}^0_f = \frac{P^0_L}{LHV_f \eta^0_{ICE}} \tag{33}$$

where P^0_L and η^0_{ICE} are the related load request and BTE. Therefore, the percentage variation in fuel consumption can be expressed as:

$$\%\Delta\dot{m}_f = \frac{\dot{m}_f - \dot{m}^0_f}{\dot{m}^0_f} \cdot 100 \tag{34}$$

and recalling equations (32) and (33), it becomes:

$$\%\Delta\dot{m}_f = \left\{ \frac{\eta^0_{ICE}}{P^0_L}\left[\frac{P_L}{\eta_{ICE}} + P^r_{HHO}\left(\frac{1}{\eta_{aux}\eta_{ICE}} - \alpha\right)\right] - 1 \right\} \cdot 100 \tag{35}$$

A qualitative representation of the overall energy flows among the considered components is given through the Sankey diagram sketched in Figure 5. Such representation refers to a generic operation and the arrows dimension should be taken as a reference example. It can be observed that the fuel represents the only inlet energy flow to the system, and the engine losses are the main cause of overall efficiency reduction. Therefore, any increase in engine efficiency can lead to a consequent reduction in fuel consumption.

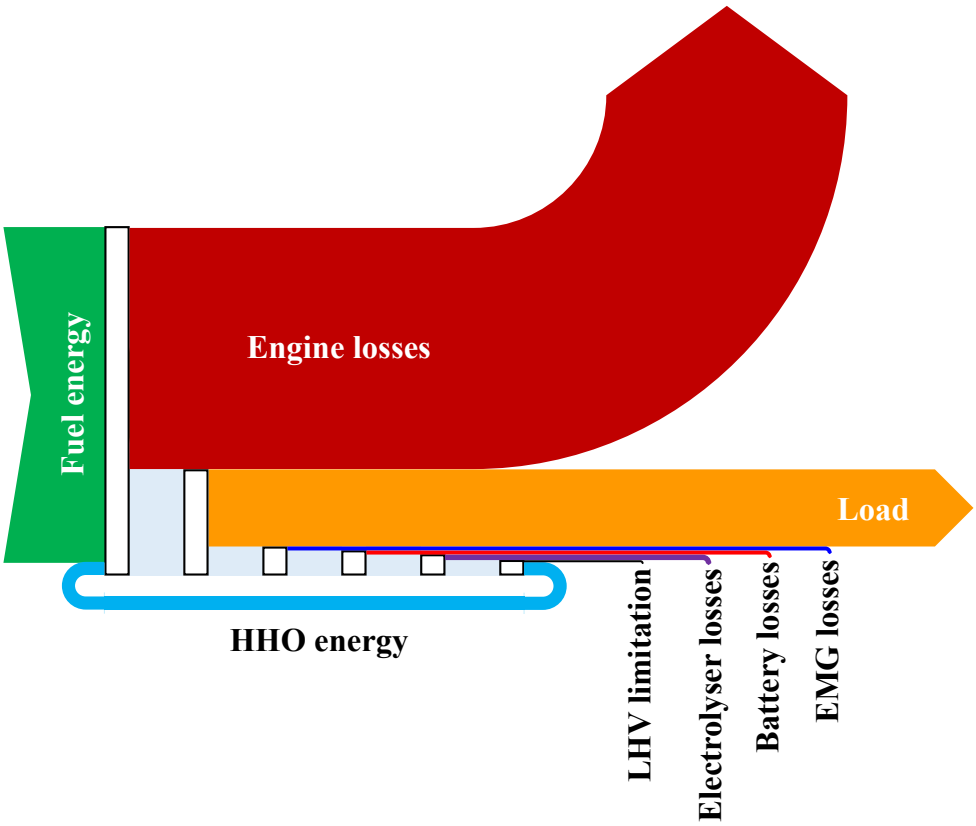

Figure 5: Qualitative Sankey diagram related to the system sketched in Figure 4.

If HHO is used to this scope, a real benefit can be achieved only if the energy amount required for HHO production is lower than the energy saved through an increase in engine efficiency. This condition is thoroughly discussed in the following section.

3.2. Fuel saving condition

Under HHO addition, the condition at which fuel saving is achieved can be clearly represented as:

$$\dot{m}_f < \dot{m}_f^0 \tag{36}$$

or in terms of percentage fuel consumption variation as:

$$\%\Delta\dot{m}_f < 0 \tag{37}$$

Recalling equation (35), equation (37) can be rearranged and expressed in terms of BTEs as follows:

$$\eta_{ICE} > \frac{\eta_{ICE}^0}{\eta_{aux}} \left(\frac{P_{HHO}^r + P_L \eta aux}{P_L^0 + \alpha P_{HHO}^r \eta_{ICE}^0} \right) \tag{38}$$

or, as well, in their percentage variation:

$$\%\Delta\eta_{ICE} > \frac{\left(P_L - P_L^0\right)\eta_{aux} + P_{HHO}^r \left(1 - \alpha\eta_{aux}\eta_{ICE}^0\right)}{\eta_{aux}\left(P_L^0 + \alpha P_{HHO}^r \eta_{ICE}^0\right)} \tag{39}$$

where:

$$\%\Delta\eta_{ICE} = \frac{\eta_{ICE} - \eta_{ICE}^0}{\eta_{ICE}^0} \cdot 100 \tag{40}$$

It can be observed that the term at the right side of equation (39) depends on the operating condition (in terms of power request and injected HHO) and components performance (in terms of engine BTE without HHO injection and auxiliaries efficiency). This term is here lumped in the parameter δ, obtaining:

$$\%\Delta\eta_{ICE} > \delta \tag{41}$$

The condition $\%\Delta\eta_{ICE} = \delta$ represents the case at which, with HHO addition, no variation of fuel consumption is achieved, i.e., $\%\Delta\dot{m}_f = 0$. Therefore, the term δ is thus named Unchanged Fuel Consumption Limit (UFCL) and represents the percentage increase in engine BTE through which the fuel consumption remains unchanged (i.e., $\dot{m}_f = \dot{m}_f^0$). Fuel saving is thus achieved if the percentage gain in BTE obtained with the addition of HHO is higher than this value, otherwise a higher fuel flow is required to cope with load request and HHO production. Noteworthy, the UFCL value does not depend on the fuel type since no information related to fuel energy content (e.g., LHV_f) is required. Therefore, this limit is only influenced by components performance, HHO flow and load request.

In the addressed literature, many authors investigate the effects of HHO injection either with fixed power request (i.e., constant torque and speed) [1, 2, 3, 9, 14, 15] or engine speed (i.e., variable torque at given speed) [4, 6, 10, 11, 12, 13, 16]. Hence, the UFCL evaluation shall be always characterized according to the considered operation.

3.2.1. Constant power operation

In this case, the power request is kept unchanged while comparing the engine performance with and without HHO addition. Therefore, the condition $P_L = P_L^0$ applies and the UFCL expression becomes:

$$\delta_{cp} = \frac{P^r_{HHO}\left(1 - \alpha\eta_{aux}\eta^0_{ICE}\right)}{\eta_{aux}\left(P^0_L + \alpha P^r_{HHO}\eta^0_{ICE}\right)} \tag{42}$$

Introducing $\kappa = P^r_{HHO}/P^0_L$ as the ratio between the power required for HHO production and the power request, equation (42) can be further simplified:

$$\delta_{cp} = \frac{1 - \alpha\eta_{aux}\eta^0_{ICE}}{\eta_{aux}\left(\frac{1}{\kappa} + \alpha\eta^0_{ICE}\right)} \tag{43}$$

From the previous equation, two limit cases can be identified focusing on η_{aux}. The first one is obtained with $\eta_{aux} = 0$, representing the extreme case at which the losses related to auxiliaries operation are predominant. At this condition $\delta_{cp} \to +\infty$, meaning that the poorer is the auxiliaries performance, the greater becomes the fuel consumption and, thus, the limit at which fuel saving can be achieved.

The opposite case is instead obtained with $\eta_{aux} = 1$, at which an ideal operation of the auxiliaries is considered. This condition is of particular interest since it represents the lowest UFCL value achievable at a given operating condition and engine performance. In this case, the UFLC value δ^{id}_{cp} is:

$$\delta^{id}_{cp} = \frac{1 - \alpha\eta^0_{ICE}}{\frac{1}{\kappa} + \alpha\eta^0_{ICE}} \tag{44}$$

A qualitative representation of δ^{id}_{cp} as function of η^0_{ICE} and κ is given in Figures 6 and 7, respectively. In these figures, the UFCL at constant power operation is represented through solid blue lines, whereas the other curves refer to the UFCL at constant speed operation (illustrated in the following section). From the trends, it can be clearly observed that the UFCL decreases with a better performing engine (i.e., at higher η^0_{ICE}), while it increases with greater amount of HHO being injected at a given power request (i.e., higher κ). In both cases, lower and upper bounds are

represented (at both left and right side y axes). With respect to Figure 6:

$$\delta_{cp}^{id}\left(\eta_{ICE}^{0}=0\right)=\kappa \tag{45}$$

$$\delta_{cp}^{id}\left(\eta_{ICE}^{0}=1\right)=\kappa\frac{1-\alpha}{1+\alpha\kappa} \tag{46}$$

the upper bound in equation (45) represents the case at which the engine losses fully absorb the inlet chemical energy of the fuel, while the lower bound in equation (46) is associated to absence of engine losses. In both cases, the limits are proportional to the amount of HHO injected as additive. Nevertheless, the right hand limit has been introduced only for mathematical analysis purposes, since the maximum theoretical engine efficiency that could be achieved is represented by the Carnot limit (dashed vertical black line).

Observing Figure 7, the following limits are shown:

$$\delta_{cp}^{id}\left(\kappa=0\right)=0 \tag{47}$$

$$\delta_{cp}^{id}\left(\kappa\rightarrow+\infty\right)\rightarrow\frac{1}{\alpha\eta_{ICE}^{0}}-1 \tag{48}$$

It is obvious that if no HHO addition is considered ($\kappa=0$), any increase in engine BTE will improve the fuel consumption. When adding HHO, the UFCL increases but its growth is limited, since for $\kappa\rightarrow+\infty$ the UFCL tends to a finite value.

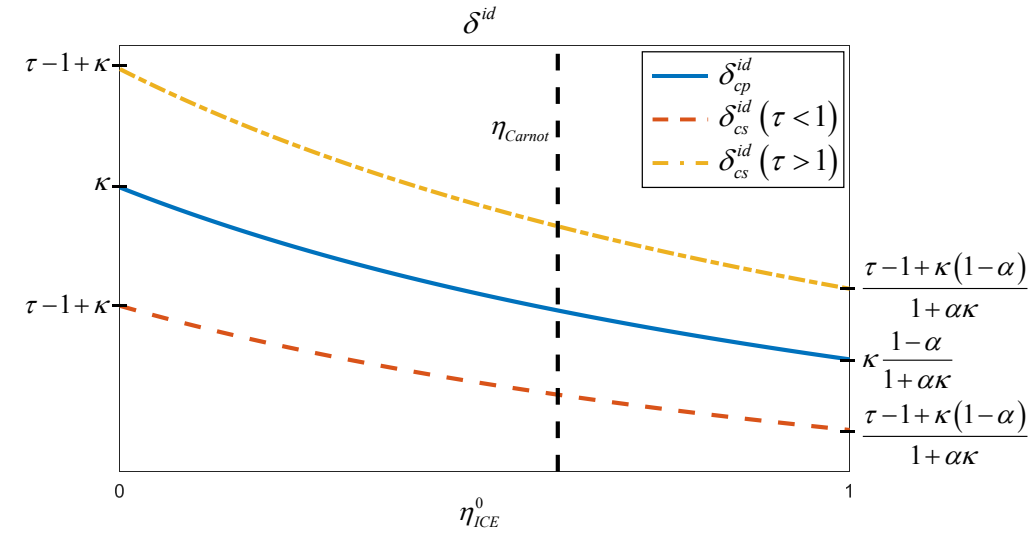

Figure 6: Qualitative representation of δ_{cp}^{id} and δ_{cs}^{id} with respect to η_{ICE}^{0}, the latter with τ higher and lower than 1.

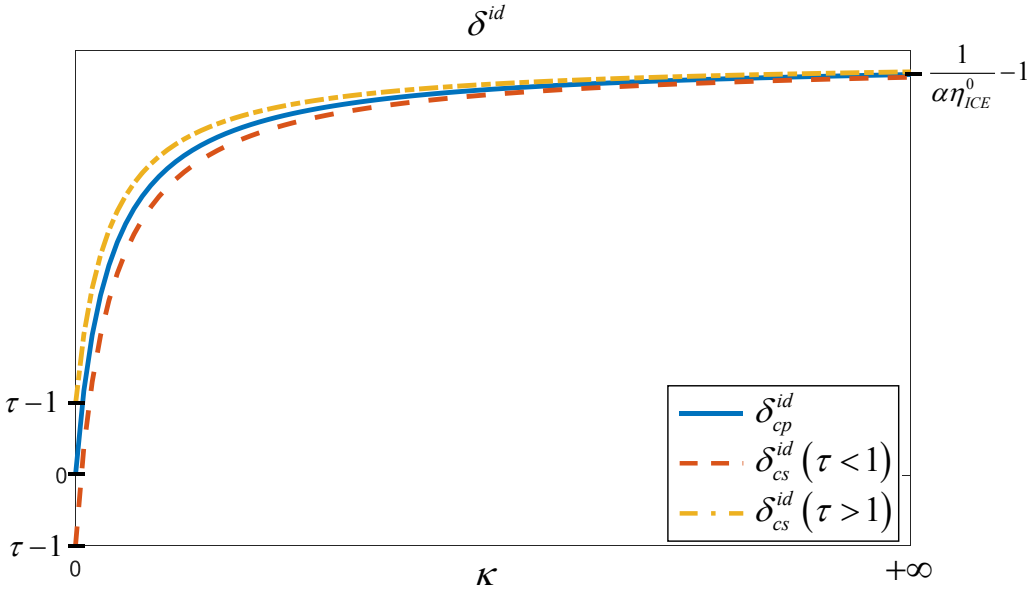

Figure 7: Qualitative representation of δ_{cp}^{id} and δ_{cs}^{id} with respect to κ, the latter with τ higher and lower than 1.

3.2.2. Constant speed operation

Differently from the previous condition of constant power, constant speed operation implies that engine performance is investigated keeping unchanged the engine speed ω, whereas engine brake torque Tq changes. In this case the following condition $\omega = \omega^0$ applies, while $Tq \neq Tq^0$. Thus, UFCL can be expressed as:

$$\delta_{cs} = \frac{\left(Tq - Tq^0\right)\omega^0 \eta_{aux} + P^r_{HHO}\left(1 - \alpha \eta_{aux} \eta^0_{ICE}\right)}{\eta_{aux}\left(Tq^0 \omega^0 + \alpha P^r_{HHO} \eta^0_{ICE}\right)} \tag{49}$$

Introducing the coefficient $\tau = Tq/Tqv^0$ and recalling equation (43) and the term κ, equation (49) becomes:

$$\delta_{cs} = \delta_{cp} + \frac{\tau - 1}{1 + \alpha \kappa \eta^0_{ICE}} \tag{50}$$

The previous equation expresses δ_{cs} as linearly dependent on δ_{cp}. The other term appearing on the right side strictly depends on the value assumed by τ, which can be either positive ($\tau \geq 1$) or negative ($\tau < 1$). Nevertheless, many authors observed that the addition of HHO brings an increase in engine torque at constant speed [4, 6, 10, 11, 13, 16], thus implying that τ is positive. This means that, at given engine performance and HHO injected amount, the UFCL can be higher if operating at constant speed rather than constant power. The previous conclusion can be motivated considering that, in such case, more torque is provided to the load, increasing the engine brake power and thus requiring more fuel.

Focusing on the auxiliaries efficiency, the limit cases with $\eta_{aux} = 0$ leads to $\delta_{cs} \to +\infty$ (since $\delta_{cp} \to +\infty$), whereas for $\eta_{aux} = 1$ the UFLC value δ^{id}_{cs} is:

$$\delta^{id}_{cs} = \delta^{id}_{cp} + \frac{\tau - 1}{1 + \alpha \kappa \eta^0_{ICE}} \tag{51}$$

As done for δ_{cp}^{id}, also δ_{cs}^{id} is qualitatively represented as function of η_{ICE}^{0} and κ in Figures 6 and 7. Also in this case, the UFCL decreases at higher η_{ICE}^{0} values, and increases with higher κ values. Lower and upper bounds are as well represented, obtaining for Figure 6:

$$\delta_{cs}^{id}\left(\eta_{ICE}^{0}=0\right)=\tau-1+\kappa \tag{52}$$

$$\delta_{cs}^{id}\left(\eta_{ICE}^{0}=1\right)=\frac{\tau-1+\kappa(1-\alpha)}{1+\alpha\kappa} \tag{53}$$

and for Figure 7:

$$\delta_{cs}^{id}\left(\kappa=0\right)=\tau-1 \tag{54}$$

$$\delta_{cs}^{id}\left(\kappa\rightarrow+\infty\right)\rightarrow\frac{1}{\alpha\eta_{ICE}^{0}}-1 \tag{55}$$

Nevertheless, the upper and lower bounds depend also on τ. If $\tau<1$, $\delta_{cs}^{id}<\delta_{cp}^{id}$, otherwise $\delta_{cs}^{id}>\delta_{cp}^{id}$ for $\tau>1$. As previously stated, τ greater than 1 implies that a higher torque is provided to the load/driveline, inducing and increase in the fuel saving limit. On the other hand, when τ is lower than 1, less torque means that less power is provided at the same speed to the load/driveline and the energy surplus is then used by the electrolyser.

In the following section, the application of the UFCL to specific case studies taken from the literature is performed, in order to assess the feasibility of running on-board HHO production systems to achieve fuel reduction.

4. Results on case studies from literature

The case studies here analysed are based on the experimental investigations reported in the works of Premkartikkumar et al. [1], Manu et al. [9], Wang et al. [3], Bari et al. [2] and Falahat et al. [13]. An overview on engine type and operation, as well as tested HHO flow rate and obtained efficiencies are reported in Table 3 for each considered work. All the parameters required for the energetic analysis can be found in Table 4, with reference to the values already reported in Tables 1 and 2 and the results illustrated in Section 2.5.

Table 3: Meaningful information and parameters related to the case studies taken from literature works.

	Ref. [1]	Ref. [9]	Ref. [3]	Ref. [2]	Ref. [13]
Fuel	Diesel	Diesel	Diesel	Diesel	Gasoline
Displacement [cc]	661	553	5883	4009	197
Operation	Constant power	Constant power	Constant power	Constant power	Constant speed
Power [kW]	5.9	3.7	24.5	[19 22 28]	up to 1.9
Speed [rpm]	1800	1500	1600	1500	[1350 1550 1750 2000 2250]
$\dot{V}_{HHO}$ [LPM]	3	2	up to 70	up to 31.7	[1 1.5 2]
η^0_{ICE} [%]	24.32	32	31.1	[32 32.9 34.7]	[20 21 21 20 19]
η_{ICE} [%]	27.01	34.99	up to 39.9	up to 36.3	up to 26

The power request for HHO production is evaluated through equation (19) upon the knowledge of HHO volumetric flow (from the literature works) and ideal energy consumption (equation (17)). The BTE increase evaluated through the literature data is firstly compared to the ideal UFCL, characterized in both pure diatomic and pure monoatomic states by means of equation (44) for constant power operation and equation (51) for constant speed operation. This analysis gives a first verification on the possibility to achieve fuel saving under the considered configuration. Afterwards, the comparison is performed with respect to a real UFCL calculated through equations (42) and (49), for constant power and constant

speed, respectively, and the corresponding fuel consumption variation is computed through equation (35).

Table 4: Parameters used for case studies verification.

Parameter	**Value**	**Unit**	**Reference**
LHV_f (Diesel)	42.61	MJ/kg	[6]
LHV_f (Gasoline)	44.79	MJ/kg	[5]
LHV_{H_2}	120.21	MJ/kg	[6]
HHV_{H_2}			see Table 2
$\bar{R}$			see Table 2
F			see Table 2
T (NTP)	293.15	[K]	[18]
p (NTP)			see Table 2
M_{H_2}	$2{\cdot}10^{-3}$	[kg/mol]	
$x^d_{H_2}$			see Table 1
$x^m_{H_2}$			see Table 1
η_{ELEC}	64	[%]	Section 2.5
η_{EMG}	87	[%]	[22]
η_{BATT}	98	[%]	[22]

The first case study is based on the work of Premkartikkumar et al. [1] that has been already discussed in Section 1. The energetic analysis is here performed assuming full power operation (i.e, constant power of 5.9 kW) with a HHO flow of 3 LPM. At this condition, the increase in BTE is about 11.06% (from the data reported in table 3). The ideal UFCL in pure diatomic state corresponds to 5.23%, whereas in pure monoatomic state it is about 2.63%. Both limits are below the

reported BTE increase, confirming the possibility to achieve a theoretical fuel consumption reduction. Assuming an auxiliary efficiency of about 54.4%, the real UFCL limits for diatomic and monoatomic states become 10.76% and 5.41%. Also in this case, the BTE percentage increase is above these limits, and the corresponding fuel consumption reductions are 0.28% (pure diatomic) and 5.12% (pure monoatomic). As discussed in Section 2.3, since the HHO mixture may behave in between the two pure states, an intermediate value should be considered. Therefore, the average fuel consumption reduction is assessed as 2.7%.

The second case study refers to the experimental investigation of Manu et al. [9], also described as the previous one in Section 1. The engine operates at a constant power of 3.7 kW with HHO flow of 2 LPM. With respect to the values reported in Table 3, the achieved BTE increase is about 9.34%, which is higher than both ideal UFCLs, that are 5.08% in pure diatomic state and 2.56% in pure monoatomics state. Hence, fuel saving is theoretically possible. However, since the real UFCLs are 10.92% and 5.51% in pure diatomic and pure monoatomic states, respectively, in the first case there is an increase in fuel consumption of about 1.47%, whereas in the second case the fuel consumption diminished of about 3.54%. Therefore, the behaviour is more prone to fuel saving, with an average fuel consumption reduction of 1.03%.

The investigation related to the third case study is based on the results carried out by Wang et al. [3], where a constant power operation (24.5 kW) and variable HHO flow rates, ranging from 0 LPM up to 70 LPM with 10 LPM steps, are applied. The comparison of the BTE increase with respect to ideal and real UFCLs under both pure diatomic and pure monoatomic states is illustrated in Figure 8-a, and the related fuel consumption variations are reported in Figure 8-b. From the

achieved results it can be observed that, for HHO flows equal or lower than 40 LPM, no fuel saving can be theoretically achieved. Both ideal UFCLs are exceeded only for HHO flows equal or higher than 60 LPM, but no proper fuel saving could be achieved when addressing real conditions. Indeed, the average fuel consumption variation, sketched as a yellow dashed line in Figure 8-b, shows a large increase with a maximum of 17.7% at 40 LPM and oscillating around 10% at higher HHO flow rates.

The engine performance changes due to HHO addition illustrated in the work of Bari et al. [2] are considered for the fourth test case analysis. As described in Section 1, the experimental investigation was performed at constant power operation with three different values, that are 19 kW, 22 kW and 28 kW. The energetic analysis results for each load value are reported in Figures 9, 10 and 11, respectively. In each figure, the comparison of the BTE increase with respect to ideal and real UFCLs (a) as well as fuel consumption variations (b) under both pure diatomic and pure monoatomic states are illustrated with respect to the specific operating condition.

The results of Figure 9-a for a constant load of 19 kW show the BTE variation almost superimposed to the ideal UFCL at pure monoatomic state. The direct consequence is the impossibility to achieve fuel saving at any investigated HHO flow rate, as proved by the results in Figure 9-b, where a linear increase in average fuel consumption is visible. Concerning results for 22 kW constant load, Figure 10-a shows that, for low HHO flow rates (below 5 LPM), fuel savings could be achieved, since the BTE increase is higher than all the reported UFCLs. Indeed, an average reduction in fuel consumption of about 1.45% is reported for a HHO flow rate of 2.5 LPM (see Figure 10-b). For higher HHO flow rates, the behaviour

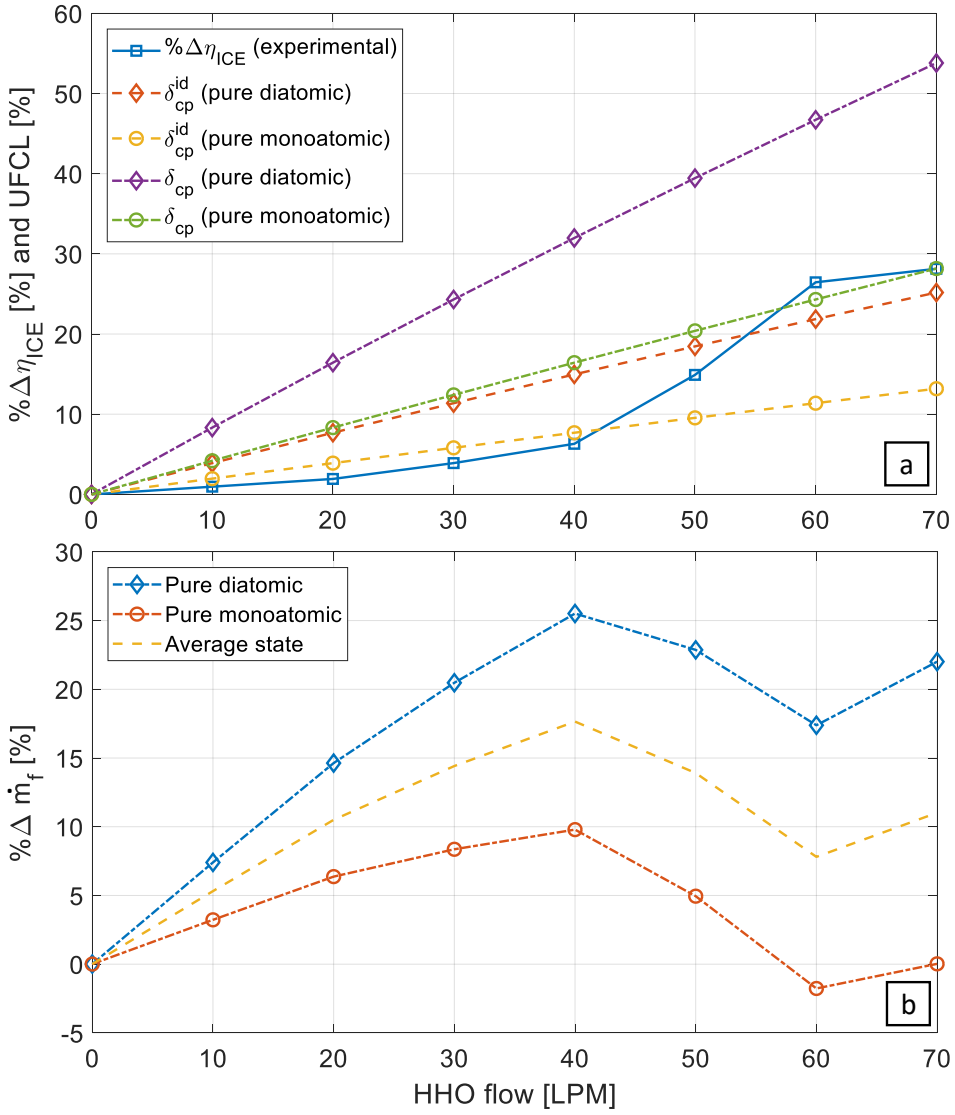

Figure 8: Comparison of the BTE increase with respect to ideal and real UFCLs in both pure diatomic and pure monoatomic states (a) and evaluation of the related changes in fuel consumption (b) for an HHO volumetric flow up to 70 LPM, based on the work of Wang et al. [3].

changes, since the BTE increase rate is lower than the increment in both ideal and real UFCLs. The 28 kW constant power condition case is instead much similar to the 19 kW case, with a BTE variation superimposed to the ideal UFCL at pure monoatomic state (Figure 11-a) and a linearly increasing average fuel consumption (Figure 11-b). Therefore, no fuel saving can be achieved at all also in this case.

The last investigated case study is related to the experimental activity carried out by Falahat et al. [13], who tested a gasoline fuelled engine at different speeds and HHO flow rates (see Table 3). In this case, the constant speed operation is thus considered and the related results are presented in Figures 12, 13 and 14 for HHO flow rates of 1LPM, 1.5 LPM and 2 LPM, respectively. Each figure illustrates the comparison of the BTE increase with respect to ideal and real UFCLs (a) as well as fuel consumption variations (b) under both pure diatomic and pure monoatomic states at different engine speeds.

For all the investigated HHO flow rates, fuel savings can be largely achieved since the BTE increase is always over the real UFCLs at any engine speed. Moreover, the higher is the HHO flow rate, the grater is the fuel consumption reduction. Nevertheless, it is worth observing that the fuel consumption reduction does not monotonically decrease with respect increasing engine speeds, but an optimal operation is observed. For 1 LPM HHO flow, a maximum reduction of about 10% is found at 1550 rpm, whereas higher values are found at 1750 rpm for both 1.5 LPM and 2 LPM HHO flow rates, that are 10.7% and 12.7%, respectively.

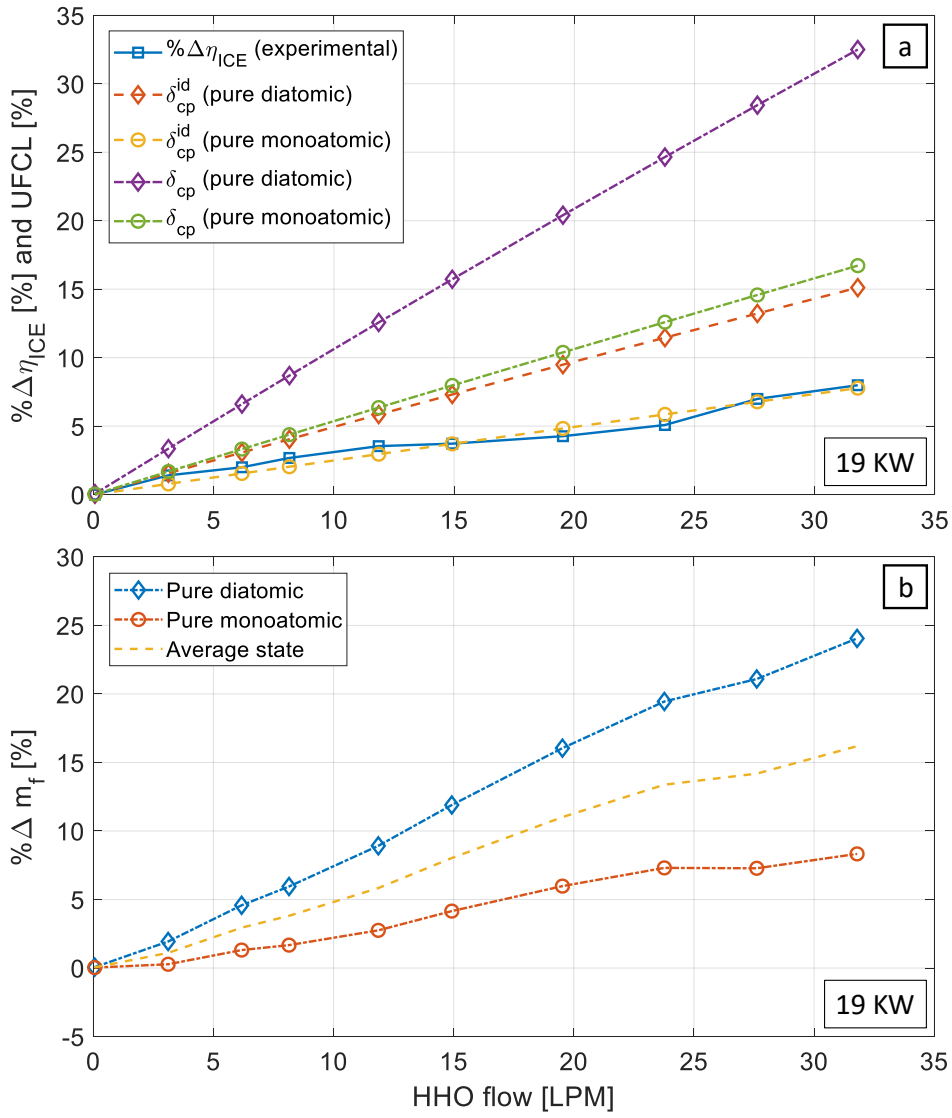

Figure 9: Comparison of the BTE increase with respect to ideal and real UFCLs in both pure diatomic and pure monoatomic states (a) and evaluation of the related changes in fuel consumption (b) for an HHO volumetric flow up to about 30 LPM at constant power of 19 kW, based on the work of Bari et al. [2].

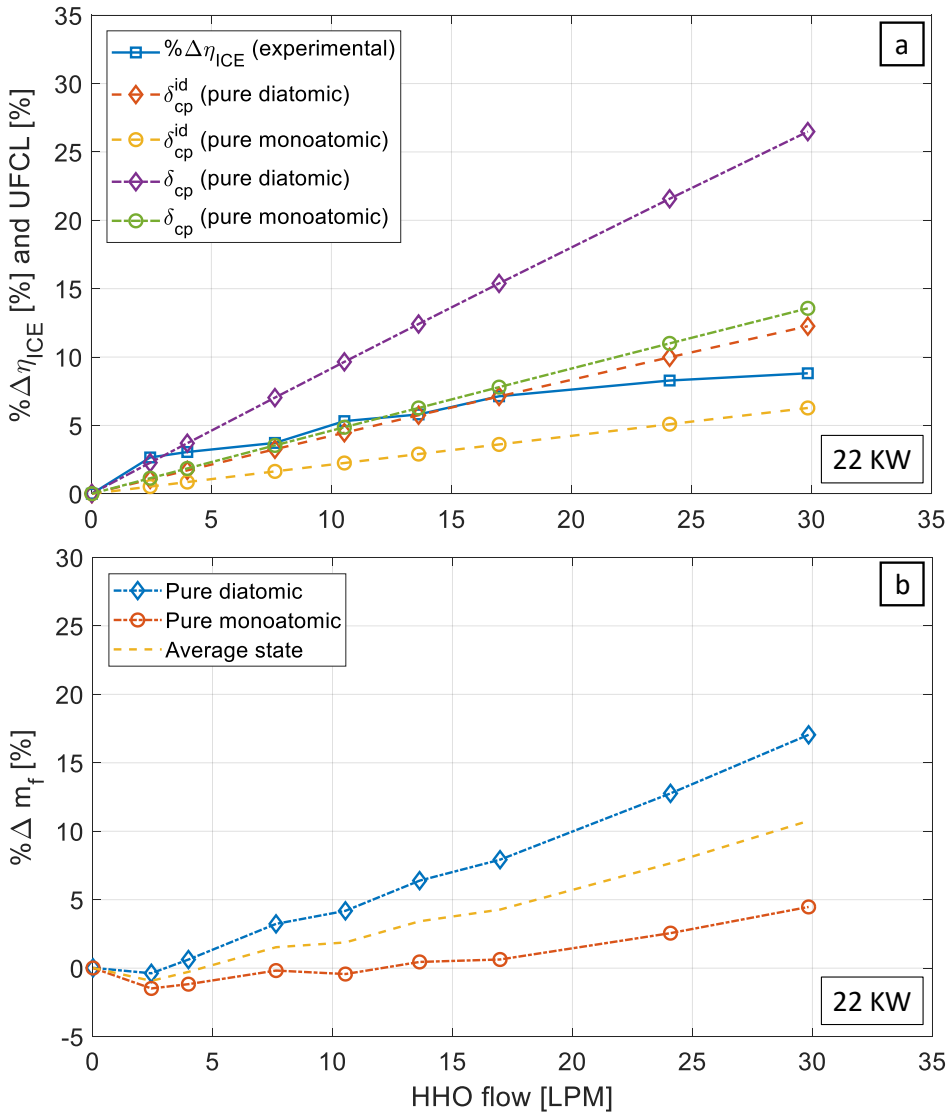

Figure 10: Comparison of the BTE increase with respect to ideal and real UFCLs in both pure diatomic and pure monoatomic states (a) and evaluation of the related changes in fuel consumption (b) for an HHO volumetric flow up to about 30 LPM at constant power of 22 kW, based on the work of Bari et al. [2].

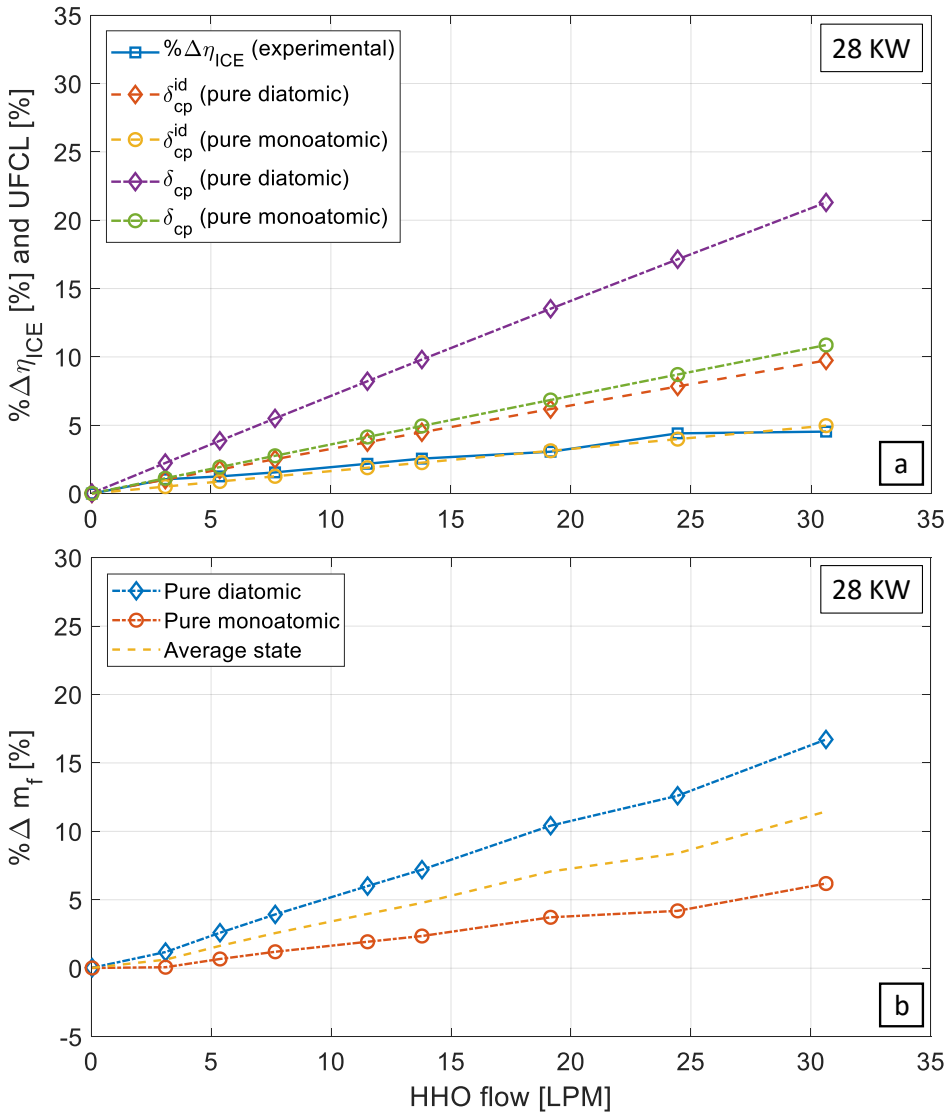

Figure 11: Comparison of the BTE increase with respect to ideal and real UFCLs in both pure diatomic and pure monoatomic states (a) and evaluation of the related changes in fuel consumption (b) for an HHO volumetric flow up to about 30 LPM at constant power of 28 kW, based on the work of Bari et al. [2].

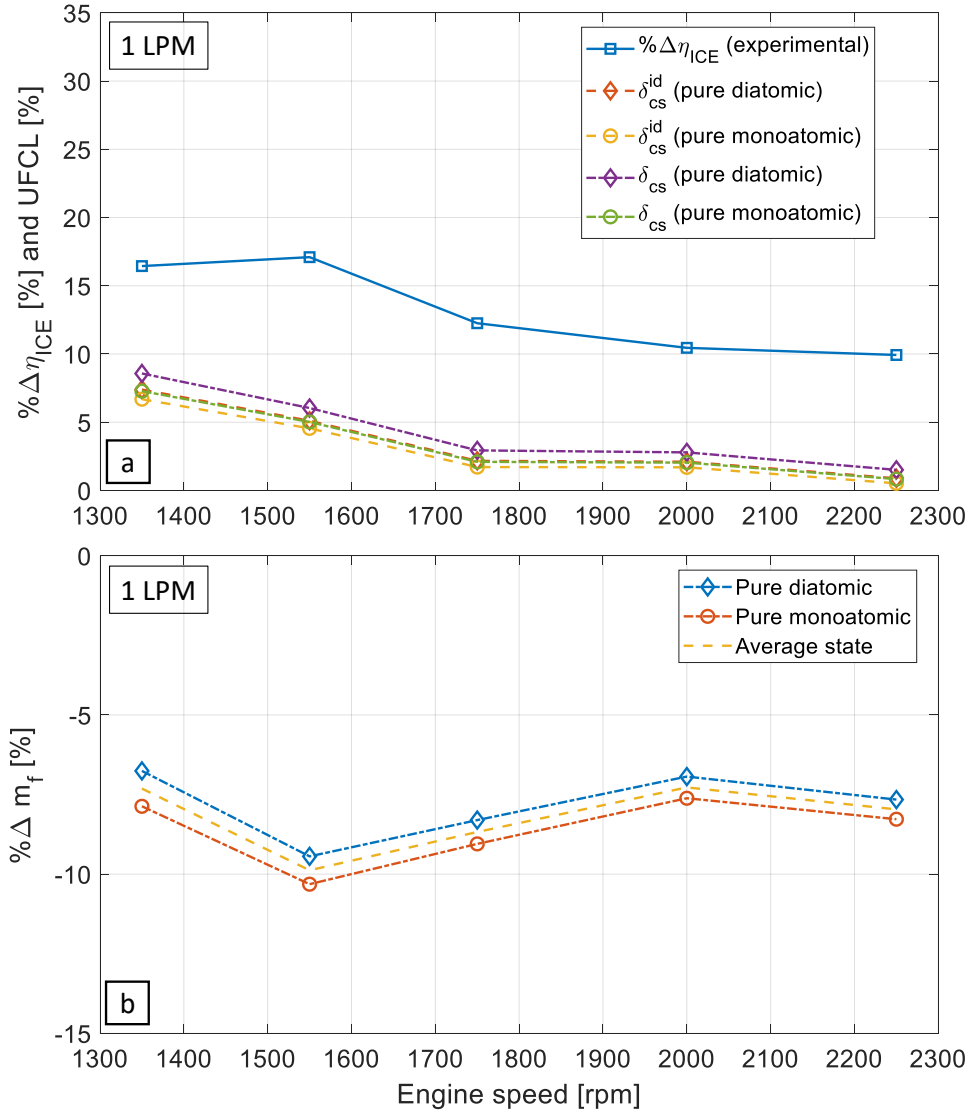

Figure 12: Comparison of the BTE increase with respect to ideal and real UFCLs in both pure diatomic and pure monoatomic states (a) and evaluation of the related changes in fuel consumption (b) for an HHO volumetric flow of 1 LPM at variable engine speeds, based on the work of Falahat et al. [13].

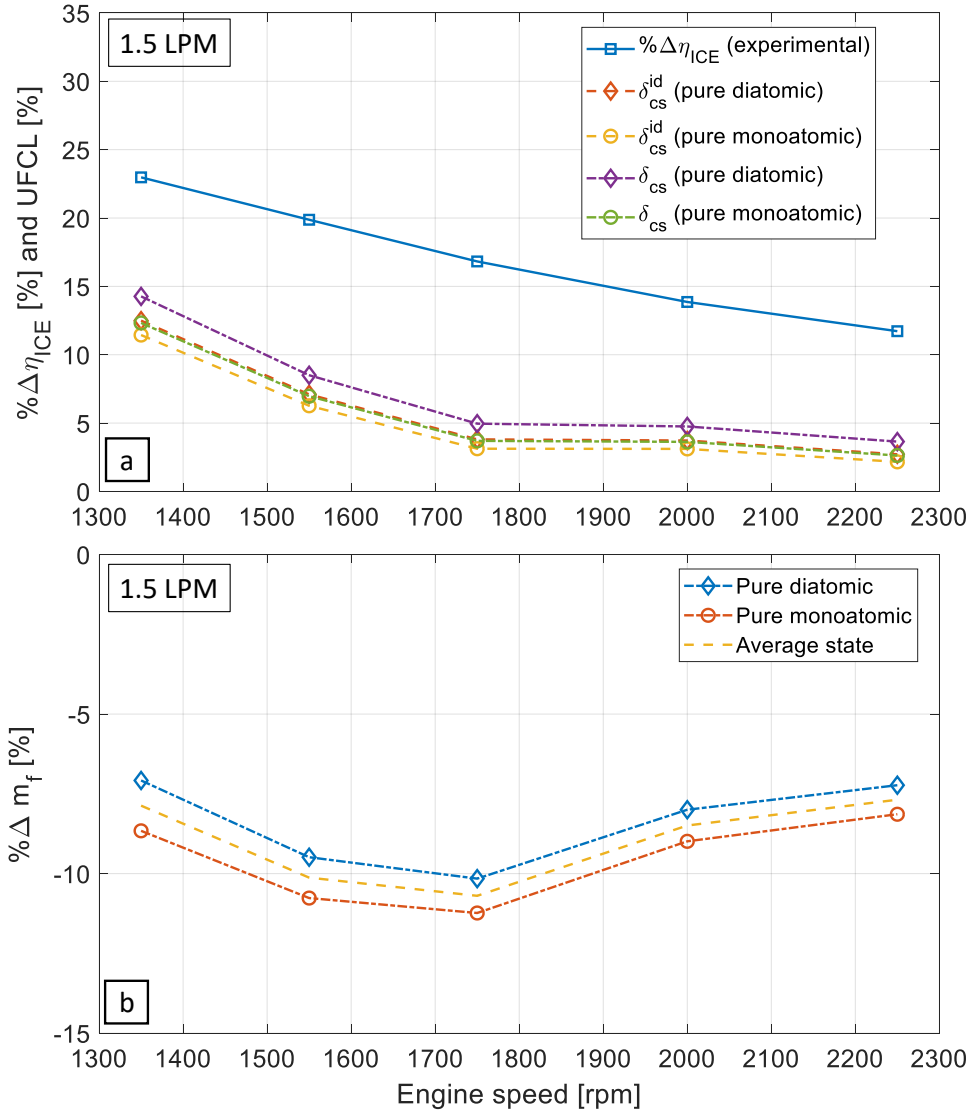

Figure 13: Comparison of the BTE increase with respect to ideal and real UFCLs in both pure diatomic and pure monoatomic states (a) and evaluation of the related changes in fuel consumption (b) for an HHO volumetric flow of 1.5 LPM at variable engine speeds, based on the work of Falahat et al. [13].

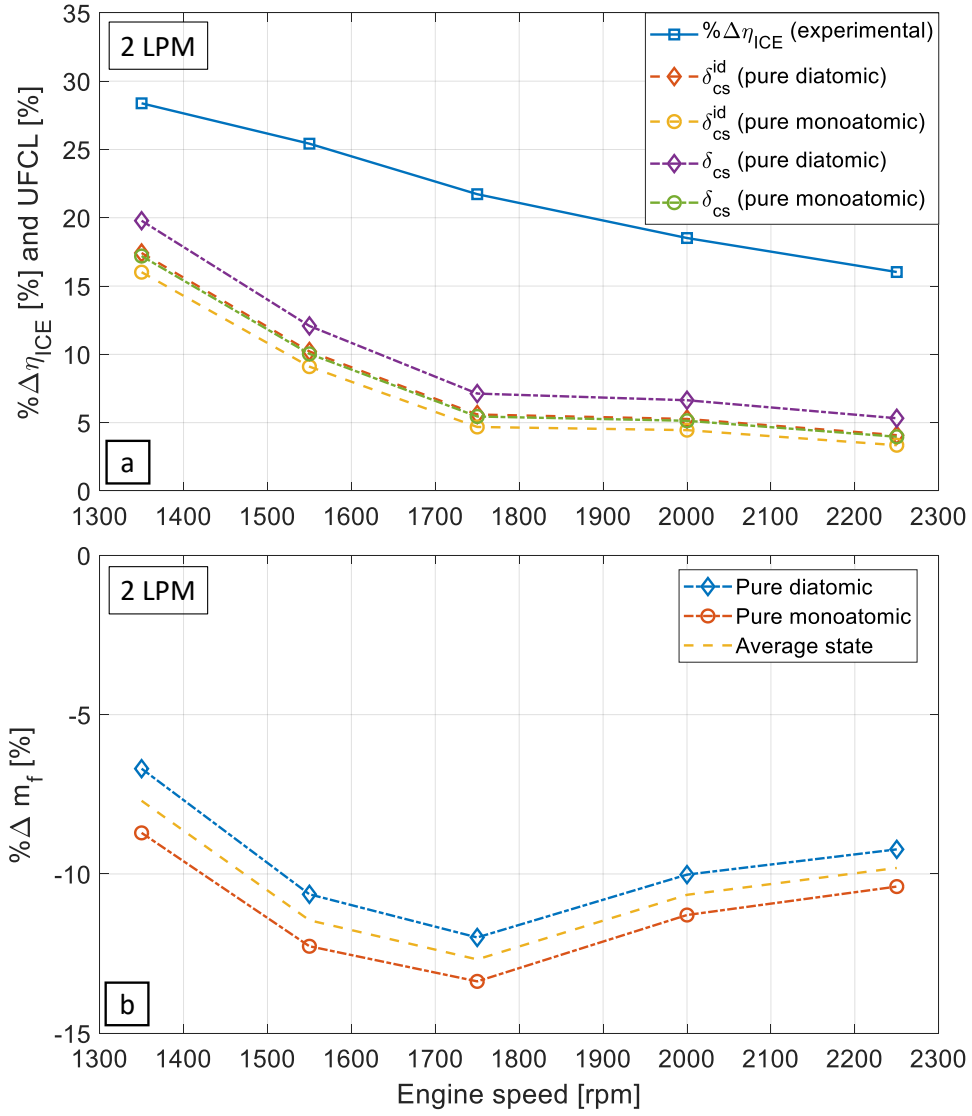

Figure 14: Comparison of the BTE increase with respect to ideal and real UFCLs in both pure diatomic and pure monoatomic states (a) and evaluation of the related changes in fuel consumption (b) for an HHO volumetric flow of 2 LPM at variable engine speeds, based on the work of Falahat et al. [13].

5. Conclusions

The present work illustrates a theoretical study on the energetic requirements related to the on-board production of Oxy-Hydrogen (HHO) for internal combustion engine systems. The main objective of this study was to assess the feasibility of using HHO under realistic operating conditions, assuming HHO produced through eletrolysis, with the electrolyser directly connected to the engine.

A thorough overview of the available literature pointed out the lack in a rigorous analysis of the whole energetic process. Several works proposed an experimental investigation of the effects related to the HHO use, reporting various efficiency increase and fuel consumption as well as emissions reduction. However, the energy required for HHO production was mainly supplied by an external power source, such as a battery, without taking power at engine output. To bridge this gap, a system layout composed by engine, electric motor generator, battery and electrolyser has been considered, assuming that the energy request for HHO production is taken at the engine shaft.

Since a univocal definition of HHO composition is not available in the literature, to properly define the gross energy demand at electrolyser inlet, an innovative assumption has been made by considering HHO a stoichiometric mixture of hydrogen and oxygen in both monoatomic and diatomic states. This assumption is proved valid by comparing computed HHO flow with the experimental findings shown by Ismail et al. [16]. It has been observed that, at low electrolysis currents, HHO seems to present more diatomic elements, whereas, at high currents, monoatomic elements seems to prevail. A further confirmation was given by the efficiency analysis, which resulted in an electrolysis efficiency of about 64%, in line with the findings of Sapountzi et al. [8].

Once defined the power request at electrolyser inlet, a rigorous analysis of the feasibility of using such device on-board has been performed. The energy links in terms of gross (required) and net (produced) power were defined for each considered component, by assuming as main constraint the useful power at engine shaft. A formulation of the fuel consumption in terms of injected HHO and useful power was defined and the corresponding fuel saving condition is achieved. A useful indicator called Unchanged Fuel Composition Limit (UFCL) has been defined, to represent through a lumped coefficient the minimum increase in engine Brake Thermal Efficiency at which no fuel consumption variation is achieved while injecting a specific amount of HHO.

The UFCL has been firstly analysed from a theoretical points of view, by addressing two different engine operations, one at constant torque and speed (i.e., power output) and the other at constant speed only. Afterwards, specific case studies have been addressed, collecting the required information from work available in the literature. Five cases have been analysed, of which four with Diesel engines operating at constant power and one with gasoline engine operating at constant speed, with various HHO flows. From the achieved results, it has been observed that with small engines and HHO flows (i.e., below 1000 cc and 5 LPM) fuel saving could be achieved, whereas this condition seems not realistic with bigger displacement and higher HHO flow rates (i.e., above 400 cc and 10 LPM). The maximum average fuel saving computed for Diesel engines is about 2.7% (for 5.9 kW and 3 LPM of HHO), whereas for gasoline engine is 12.7% (for 1750 rpm and 2 LPM of HHO).

From these results, it can be stated that fuel savings could be achieved through on-board HHO production and injection by taking useful energy directly form the

engine. Nevertheless, a proper reduction in fuel consumptions may not always be possible since it strictly depends on different factors: i) the considered system (i.e., being a Diesel or a gasoline fuelled engine with a specific displacement), ii) the operating condition (i.e., constant load or speed) and the amount of injected HHO. As also observed in other literature works, although theoretically possible, proper fuel savings can be practically achieved upon suitable management of engine operation and HHO injection, such as the optimization of pressure ratio and spark advance.

Further activities that can be performed in the future will entail the detailed modelling of the effects of HHO addition inside the combustion chamber and the performance of dedicated experimental tests to investigate fuel consumption variation with the engine equipped with an on-board HHO generator.

Nomenclature

Acronyms

BTE Brake Thermal Efficiency

CI Compression Ignition

CNG Compressed Natural Gas

ECU Electronic Control Unit

EMG Electric Motor Generator

HER Hydrogen Evolution Reaction

HHO Oxy-Hydrogen

HHV Higher Heating Value

ICE Internal Combustion Engine

LHV Lower Heating Value

LPG Liquefied Petroleum Gas

NTP Normal Temperature and Pressure

OER Oxygen Evolution Reaction

SFC Specific Fuel Consumption

SI Spark Ignition

STP Standard Temperature and Pressure

UFCL Unchanged Fuel Consumption Limit

Greek Symbols

δ UFCL [-]

η efficiency [-]

κ HHO to load power ratio [-]

ω engine speed [rad s^{-}1]

ρ density [kg m^{-}3]

τ torque ratio [-]

ε energy consumption per unit of volume [J m^{-3}]

ζ diatomic molecules fraction [-]

Roman Symbols

$\bar{R}$ Ideal gas constant [J mol^{-1} K^{-1}]

$\dot{m}$ Mass flow [kg s^{-1}]

$\dot{n}$ Molar flow [mol s^{-1}]

F Faraday's constant [C mol^{-1}]

HHV Higher Heating Value [J kg^{-}1]

I Current [A]

LHV Lower Heating Value [J kg^{-1}]

M Molar mass [g mol^{-1}]

n Moles [mol]

N_c Electrolyser cells number [-]

P Power [W]

p Pressure [Pa]

T Temperature [K]

Tq Torque [N m]

V Volume [m^3]

Superscripts

g gross

id ideal

r request

0 no HHO addition

Subscripts

aux auxiliaries

$BATT$ battery

$chem$ chemical

cp constant power

cs constant speed

$ELEC$ electrolyser

EMG Electric Motor Generator

f fuel

H_2 hydrogen

H_2O water

HHO Oxy-Hydrogen

ICE engine

L load

References

[1] S. Premkartikkumar, K. Annamalai, A. Pradeepkumar, Effectiveness of oxygen enriched hydrogen-hho gas addition on direct injection diesel engine performance, emission and combustion characteristics, Thermal Science 18 (2014) 259–268. doi:10.2298/TSCI121014078P.

[2] S. Bari, M. Mohammad Esmaeil, Effect of h2/o2 addition in increasing the thermal efficiency of a diesel engine, Fuel 89 (2010) 378–383. doi:10.1016/j.fuel.2009.08.030.

[3] H. Wang, C. Cheng, K. Chen, Y. Lin, C. Chen, Effect of regulated harmful matters from a heavy-duty diesel engine by h2/o2 addition to the combustion chamber, Fuel 93 (2012) 524–527. doi:10.1016/j.fuel.2011.11.034.

[4] A. Yilmaz, E. Uludamar, K. Aydin, Effect of hydroxy (hho) gas addition on performance and exhaust emissions in compression ignition engines, International Journal of Hydrogen Energy 35 (2010) 11366–11372. doi:10.1016/j.ijhydene.2010.07.040.

[5] P. Pakale, N. Pawar, H. Patil, S. Patel, Efficiency improvement of si/ci engine by using blend of oxy-hydrogen gas with fuel, International Journal of Research in Advent Technology 3 (2015) 51–59.

[6] H. Arat, M. Baltaciolu, M. Özcanli, K. Aydin, Effect of using hydroxy - cng fuel mixture in a non-modified diesel engine by substitution of diesel fuel, International Journal of Hydrogen Energy 41 (2016) 8354–8363. doi:10.1016/j.ijhydene.2015.11.183.

[7] A. de Morais, M. Justino, O. Valente, S. de Morais Hanriot, J. Sondré, Hydrogen impacts on performance and co2 emissions from a diesel power generator, International Journal of Hydrogen Energy 38 (2013) 6857–6864. doi:10.1016/j.ijhydene.2013.03.119.

[8] F. Sapountzi, J. Gracia, C. Weststrate, H. Fredriksson, J. Niemantsverdriet, Electrocatalyst for the generation of hydrogen, oxygen and synthesis gas, Progress in Energy and Combustion Science 58 (2017) 1–35. doi:10.1016/j.pecs.2016.09.001.

[9] P. Manu, A. Sunil, S. Jayaraj, Experimental investigation using an on-board dry cell electrolyzer in a ci engine working on dual fuel mode, Energy Procedia 90 (2016) 209–216. doi:10.1016/j.egypro.2016.11.187.

[10] A. Sakhrieh, A. Al-Hares, F. Faqes, A. Al Baqain, N. Alrafie, Optimization of oxyhydrogen gas flow rate as a supplementary fuel in compression ignition combustion engines, International Journal of Heat and Technology 35 (2017) 116–122. doi:10.18280/ijht.350116.

[11] H. Masjuki, A. Ruhul, N. Mustafi, M. Kalam, M. Arbab, I. Rizwanul Fattah, Study of production optimization and effect of hydroxyl gas on a ci engine performance and emission fueled with biodiesel blends, International Journal of Hydrogen Energy 41 (2016) 14519–14528. doi:10.1016/j.ijhydene.2016.05.273.

[12] S. Musmar, A. Al-Rousan, Effect of hho gas on combustion emissions in gasoline engines, Fuel 90 (2011) 3066–3070. doi:10.1016/j.fuel.2011.05.013.

[13] A. Falahat, M. Hamdan, J. Yamin, Engine performance powered by a mixture of hydrogen and oxygen fuel obtained from water electrolysis, International Journal of Automotive Technology 15 (2014) 97–101. doi:0.1007/s12239-014-0011-0.

[14] N. Patil, C. Chavan, A. More, P. Baskar, Generation of oxy-hydrogen gas and its effect on performance of spark ignition engine, IOP Conference Series: Materials Science and Engineering 263 (2017) 062036. doi:10.1088/1757-899X/263/6/062036.

[15] S. Premkartikkumar, Influence of oxygen enriched hydrogen gas as a combustion catalyst in a di diesel engine operating with varying injection time of a diesel fuel, RCS Advances 5 (2015) 30583–30591. doi:10.1039/c5ra00075k.

[16] T. Ismail, K. Ramzy, M. Abelwhab, B. Elnaghi, M. Abd El-Salam, Performance of hybrid compression ignition engine using hydroxy (hho) from dry cell, Energy Conversion and Management 155 (2018) 287–300. doi:10.1016/j.enconman.2017.10.076.

[17] N. Alam, K. Pandey, Experimental study of hydroxy gas (hho) production with variation in current, voltage and electrolyte concentration, IOP Conference Series: Materials Science and Engineering 225 (2017) 012197. doi:10.1088/1757-899X/225/1/012197.

[18] J. Wright, A. Johnson, M. Moldover, Design and uncertainty analysis for a pvtt gas flow standard, Journal of Research of the National Institute of Standards and Technology 108 (2003) 21–47. doi:10.6028/jres.108.004.

[19] Iupac compendium of chemical terminology, http://goldbook.iupac.org, Accessed: 2018-02-17.

[20] R. Santilli, A new gaseous and combustible form of water, International Journal of Hydrogen Energy 31 (2006) 1113–1128. doi:10.1016/j.ijhydene.2005.11.006.

[21] F. D'Aniello, P. Polverino, I. Arsie, C. Pianese, Energetic analysis of oxy-hydrogen injection in internal combustion engines., Proceedings of EFC2017 European Fuel Cell Technology and Applications Conference - Piero Lunghi Conference, December 12-15, 2017, Naples, Italy.

[22] L. Guzzella, A. Sciarretta, Vehicle Propulsion Systems: Introduction to Modeling and Optimization, Springer, 2005.